1968-05

Stresses developed on the surface of cylindrical joints subjected to multiple loads.

Schaff, James Carl

Monterey, California. Naval Postgraduate School

STRESSES DEVELOPED ON THE SURFACE OF CYLINDRICAL JOINTS SUBJECTED TO MULTIPLE LOADS

James Carl Schaff

Dr. W. M. Murray

May 17, 1967

STRESSES DEVELOPED ON THE SURFACE OF CYLINDRICAL JOINTS SUBJECTED TO MULTIPLE LOADS

by

JAMES CARL SCHAFF

LIEUTENANT, UNITED STATES NAVY

B.S.E.E., University of Washington

(1962)

Submitted in Partial Fulfillment of the

Requirements for the Degree of

Naval Engineer and the Degree of

Master of Science in Naval Architecture

and Marine Engineering

at the

MASSACHUSETTS INSTITUTE OF TECHNOLOGY

May, 1968

Signature of Author: James Carl Schaff

Department of Naval Architecture and Marine Engineering, May 17, 1968

Certified by: W. M. Murray

Thesis Supervisor

Certified by: _____

Departmental Reader

Accepted by: _____

Chairman, Departmental Committee on Graduate Students

ABSTRACT

STRESSES DEVELOPED ON THE SURFACE OF CYLINDRICAL JOINTS SUBJECTED TO MULTIPLE LOADS

James Carl Schaff

Submitted to the Department of Naval Architecture and Maring Engineering on May 17, 1968 in partial fulfillment of the requirements for the Master of Science degree in Naval Architecture and Marine Engineering and the Professional Degree, Naval Engineer.

This paper deals with the stresses developed at the intersection of teo circular members of different diameters. Both members carried axial loads, with the larger member being continuous through the connection and the smaller terminating at the connection. The method for determination of the stress was by coating the larger member with photoelastic plastic and observing the stresses that developed at the connection. Stress concentration factors were determined by loading the larger member prior to the connecting of the smaller members.

Analytical results, obtained from attempting to predict the moment in the larger member generated by the load on the smaller member, were calculated by using Hovgaard's Continuous Ring Frame Analysis and Hardy Cross's Column Analogy. The circumferential stress from this moment was combined with the axial stress from the large member's end load, and the result modified by the stress concentration factor determined earler. When the model tests were compared to the analytical results, it was found that the moment or stress predicted was 2.5 to 3.2 times higher than that which would be expected from the model tests. A great deal more investigation must be done with this type of joint before a clear understanding of what is happening within both members will be reached.

Thesis Supervisor: Dr. W. M. Murray
Title: Professor of Mechanical Engineering

INDEX

FIGURE I

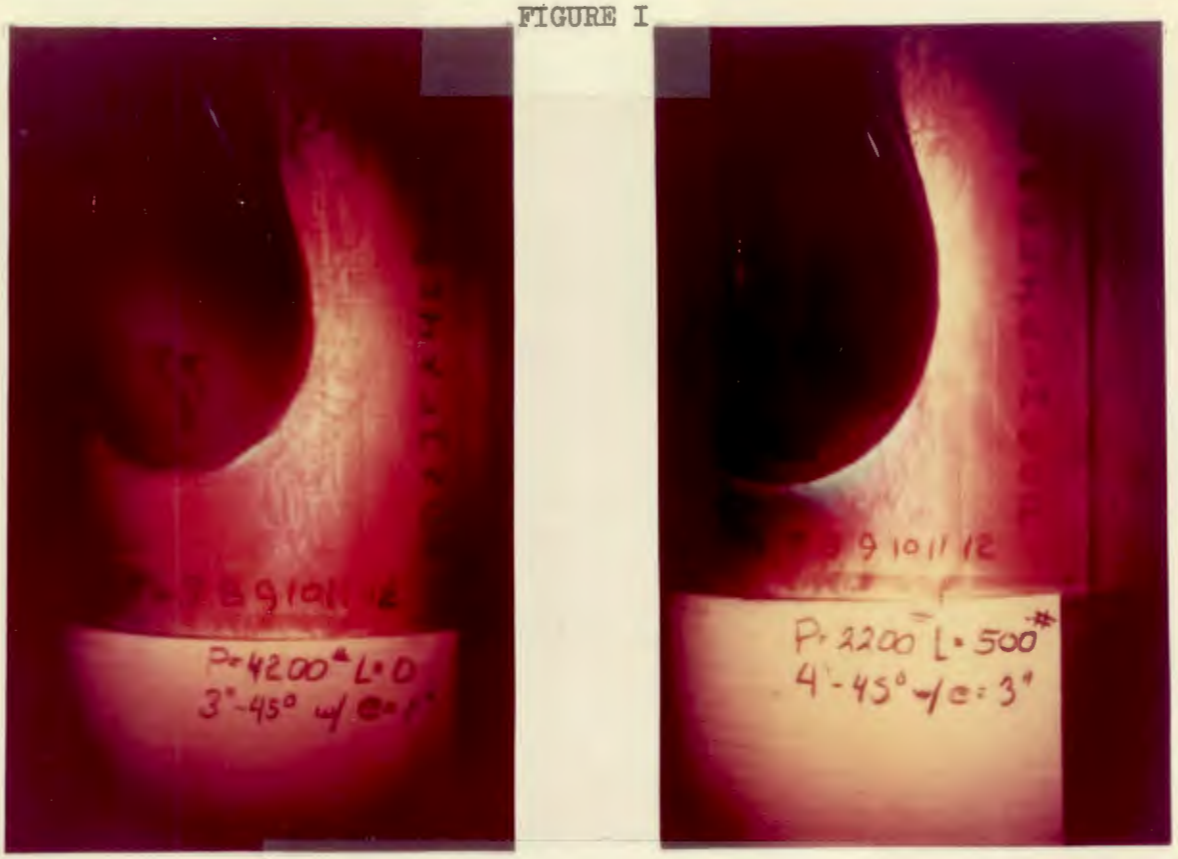

MODELS UNDER TESTING CONDITIONS

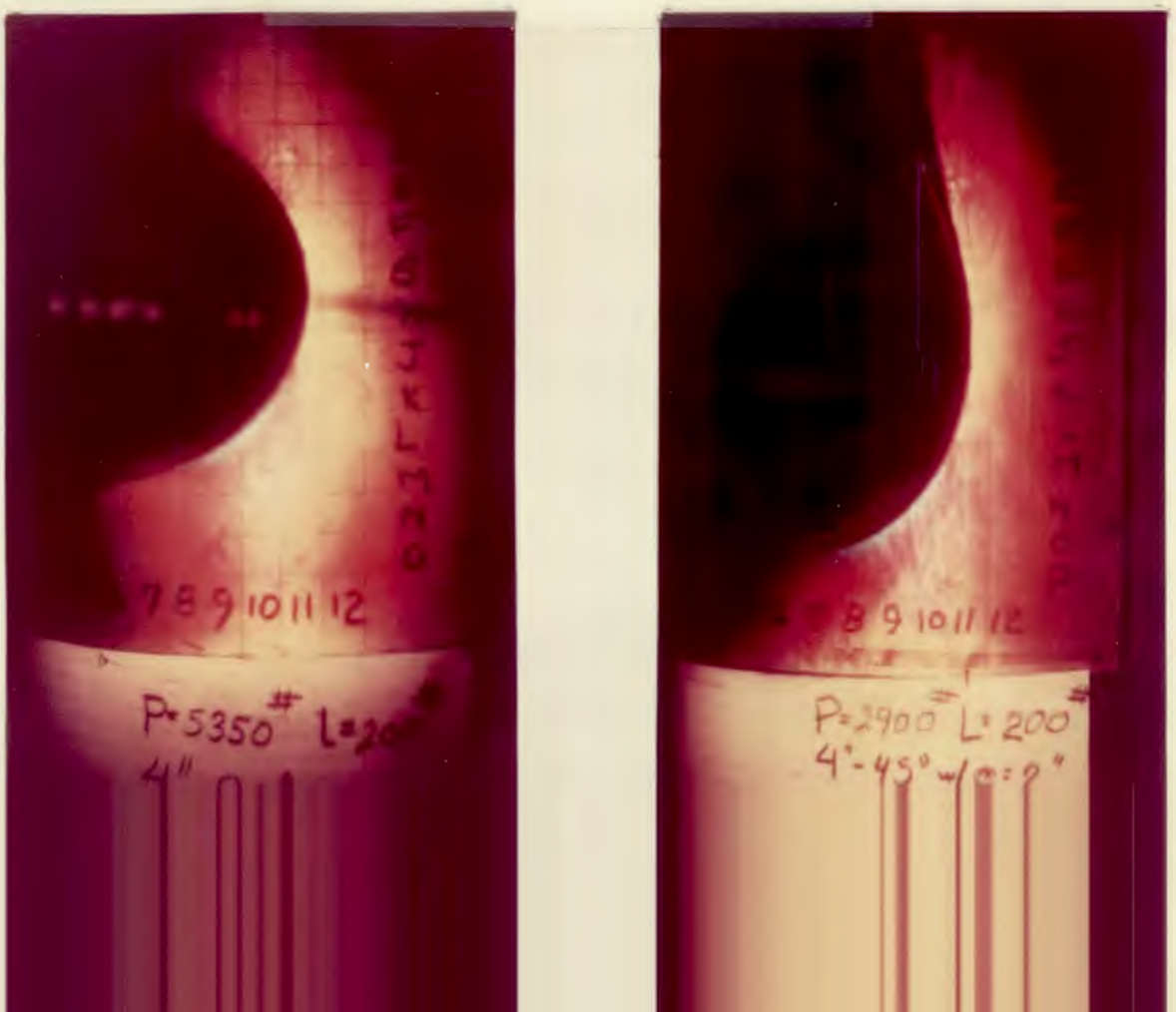

FIGURE II

MODELS UNDER TESTING CONDITIONS

INTRODUCTION

While doing research for a paper on Column Stabilized Ocean Platforms, the methods of the structural analysis was of the greatest interest to me. It was noted that several of the ocean drilling platforms in the Gulf of Mexico were lost during storms over the past few years, due to structural failures. Although the loss of these platform were attributed to the fact that they were struck by storms more severe than anticipated in the designs, an interesting aspect was, that most failures occured in the area of the connection between the main bouyant or support column and the smaller structural braces.*[12] **

It is my intension in this Thesis to investagate the stresses developed in the cord. The area of investagation will be points along a line described by the intersection of the cord and the branch, see Figure III.

The literature search revealed that the normal method for analysing this type of joint is to take the actual three dimensional case and reduce it to a two dimensional case. The stresses in the main cord due to the loading of the cord are treated separately from the stresses developed in the cord due to load on the branch. These two loads are thus combined by Mohr's Circle Method to determine the stress magnitude within the cord itself. The problem as always is whether a two dimensional analysis of a three dimensional case produces accurate or sufficent results.

---

* During the course of this Thesis the main large column will be refered to as the "Cord". The secondary small column or structural braces will be refered to as the "Branch".

** Numbers in brackets refer to references in the appendix.

FIGURE III

AREAS OF INVESTIGATION

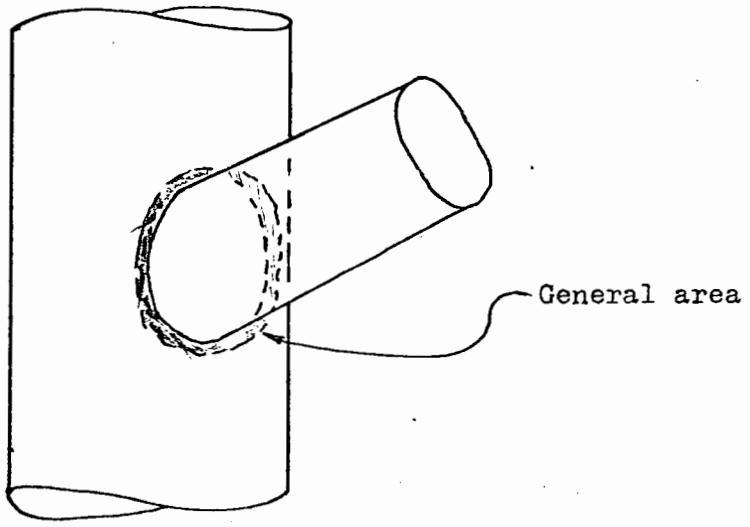

Specific Areas and Numbering System

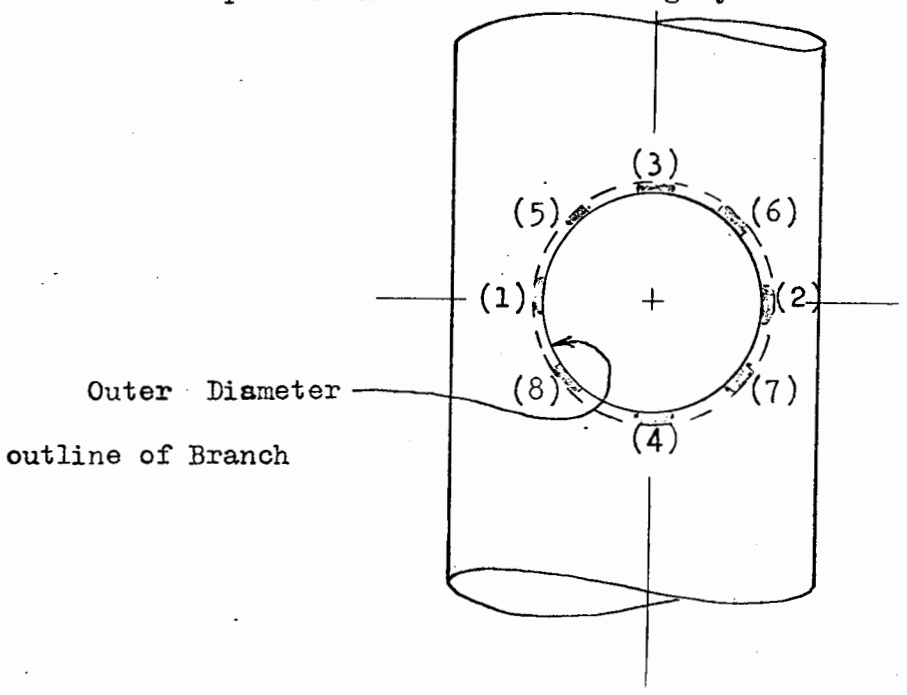

Normal analysis of the stresses introduced into the cord by the branch can be done by one of three methods: Hardy Cross's Column Analogy [11], Horgaard's Ring Frame Analyses [3], or by using a computer program such as Strudle or Stress. All three of these approaches will give approximately the same results if the same two dimensional model is used. With these methods of analysis several questions arise. The first as previously mentioned is whether a three dimensional situation can be accurately modeled in two dimensions. The analysis mentioned above takes the total branch load and applies it as two point loads as shown in Figure IV. This is questionable in that the actual load distribution is uniformly around the circumference of the branch. A second question is, where to apply the reactions R_1 and R_2 to the branch load, see Figure IV. For any of these analyses to be used the two dimensional representation must be in static equilibrium. This requires equal and opposite reactions to be applies to the cord, but where? Finally these analysis fail to take into account any effect that applying a branch has on the stiffness of the cord.

The question of the validity of this type of analysis, and therefore the question to be answered in this Thesis, reduces to one of; does the above analysis give sufficient results? It is reconized that the analysis will give only the stress distribution on one circumference of the cord and that the maximum stresses may well appear at some other circumference or point. But does the maximum stress predicted by this type of analysis exceed, equal, or is less than the actual maximum stress no matter where it occures.

The method for obtaining data was as follows; models were constructed

FIGURE IV

METHOD OF ANALYSIS OF BRANCH LOAD

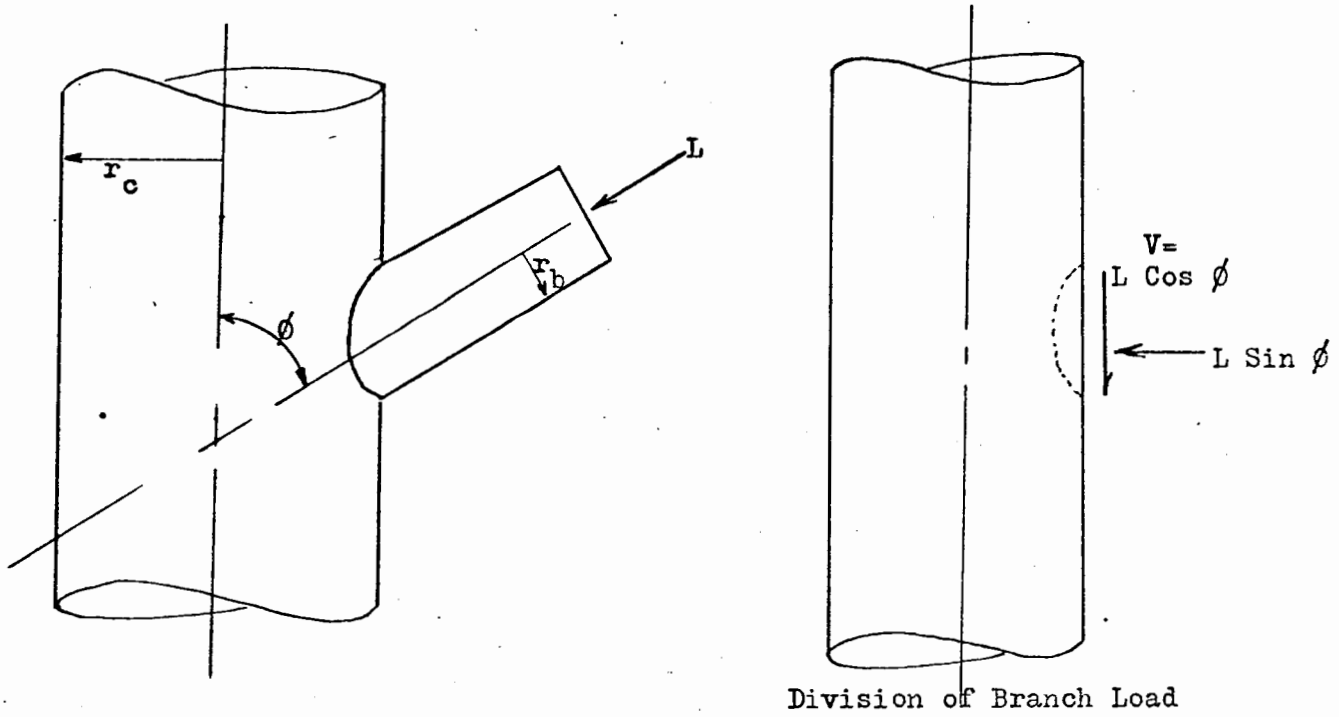

Division of Branch Load

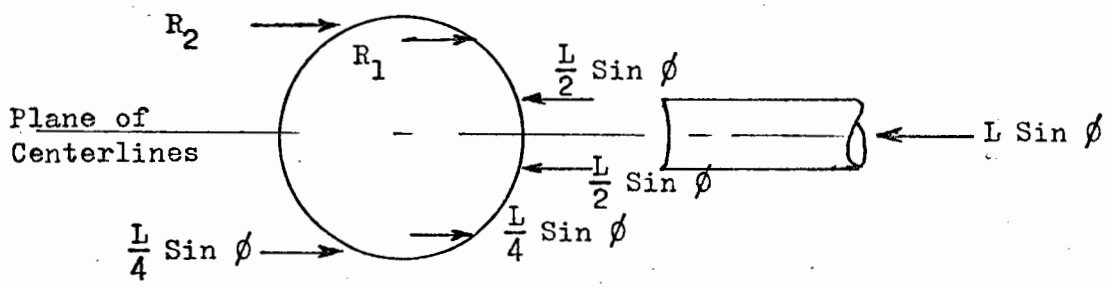

2 - Dimensional Model used in Analyses

of this type of joint using Polyvinyl Choride Pipe in a variety of configurations, see Figure V . Data was gathered from these models as to the loads which produced a given magitude of principal stress differences at a variety of locations within the area. Analysis was carried out using existing procedures, and these results were compared with data obtained from the models.

FIGURE V

THREE OF THE FOUR MODELS TESTED

4 Inch 45°

3 Inch 90°

4 Inch 90°

PROCEDURE

Polyvinyl Chloride Pipe was used to make the models of the cylindrical joints. The cords were eight inches in diameter with two size branches, three inches and four inches in diameter, being connected at 45° and 90° angles to the centerline of the cord.

Polyvinyl Chloride pipe was used because of its exhibiting approximately the same modulus of elasticity as the photoelastic plastic coating. This eliminated the need of calculating any reinforcing effect that the plastic may have on the models. The wall thickness of the model was then taken as the thickness of the Polyvinyl Chloride pipe plus the plastic coating. Using this method the stress readings are not those developed on the surface of the model as with normal photoelastic models, but an average stress through the thickness of the plastic coating, see Figure VI .

The models were constructed in the following manner; the plastic coating was cast in sheets and contoured to the pipe, after hardening, the coating was removed and cemented to the pipe with reflective cement. Only the cords were coated with plastic for only the stress developed within the cords were investigated. The plastic was applied contineously around the cord, in three or four sheets, to maintain approximately uniform thickness of the wall. The multiple sheets were necessary due to the limited size of the casting plate. The branches were cut so that they were contoured to the cord. The cords were contineous through the connection with the branch and the branch was cemented directly to the plastic coating.

Data was taken in the following manner; first the cords were loaded with a variety of axial forces, end moment, and with no branch load to

FIGURE VI

STRAIN MAGITUDES SEEN IN PHOTOELASTIC MODELS

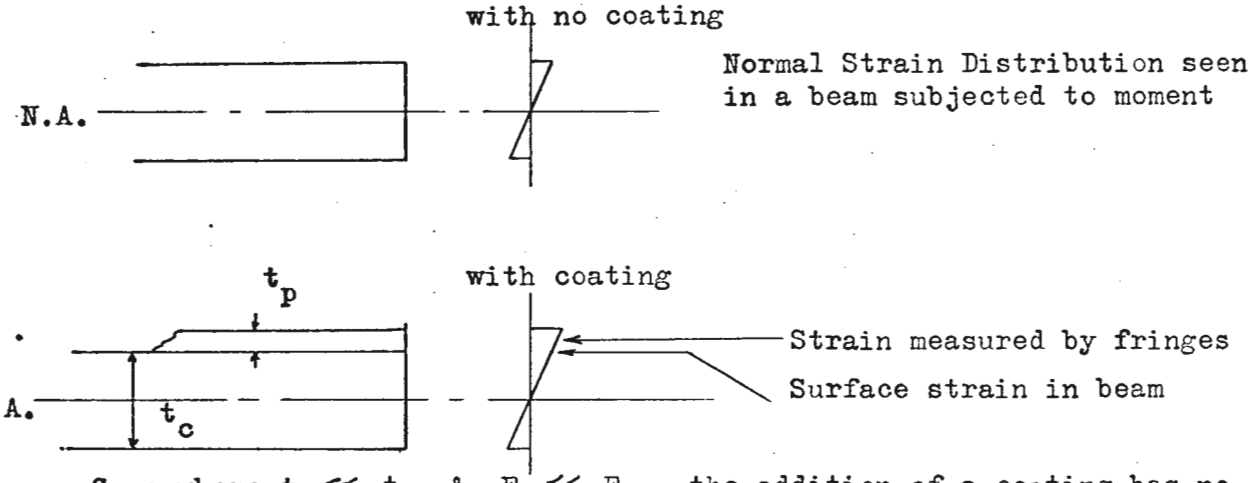

Case where $t_p \ll t_c$ & $E_p \ll E_c$, the addition of a coating has no stiffness and therefore no shift in N.A.

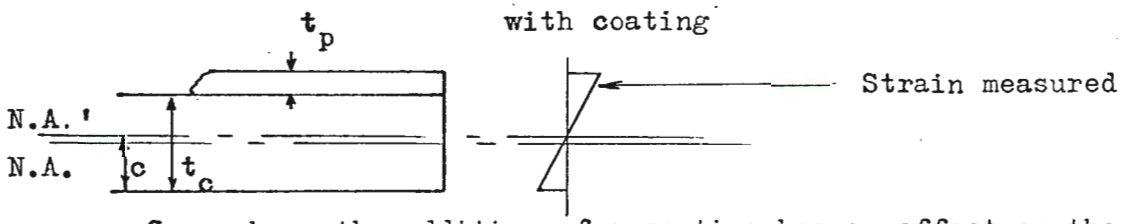

Case where the addition of a coating has an effect on the N.A. but $E_p \neq E_c$ and therefore $c < (t_p+t_c)/2$ and the reinforcing effect must be figured.

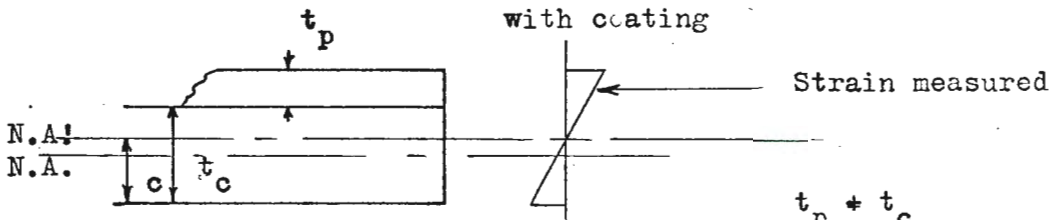

Case where $E_p = E_c$ and therefore $c = \frac{t_p + t_c}{2}$ and the strain measured is the average through the thickness of the coating t_p.

determine the effect that the application of the brnach had on the strength or rigidity of the cord. After these base points were established the branches were loaded axially and the cord loads repeated. Data was taken on the appearance of the fringes at a variety of locations in the cord where the branch was cemented to the cord. These locations were as in Figure III.

Mathematical analysis was carried out by the present hypothesis that the cord and branch loads can be treated independently, then added together by Mohr's Circle methods. Both Hovgaard's Ring Frame Analyses and Hardy Cross's Column Analogy methods were used to determine the stresses generated by the branch loads in the cord. In both of these methods the reactions R_1 and R_2 was applied at different locations to determine this effect on the stress generated at the connection. Also the amount of load L was left as a variable in order to determine whether all or a portion should be used as point loads in these analyses. The reinforcing effect of the application of the branch to the cord, as determined in the model tests, was multipled times the stress calculated above. This final stress was compared to that determined in the model tests. In the case of the branch at a 45° angle with the cord centerline, two branch loads were treated and analized. The axial branch load was broken into two equal loads being transmitted to the cord, one being a load perpendicular to the cord centerline an with the 90° branch and the second as a shear load acting on the surface of the cord. The shear component was taken as a load per distance of the circumference of the branch and treated as a pure shear at the sides and pure compression or tension at the bottom or top of the area investigated.

FIGURE VII

CONNECTION OUTLINE AND AREAS OF INVESTIGATIONS

MODELS WITH $\phi = 90^{\circ}$

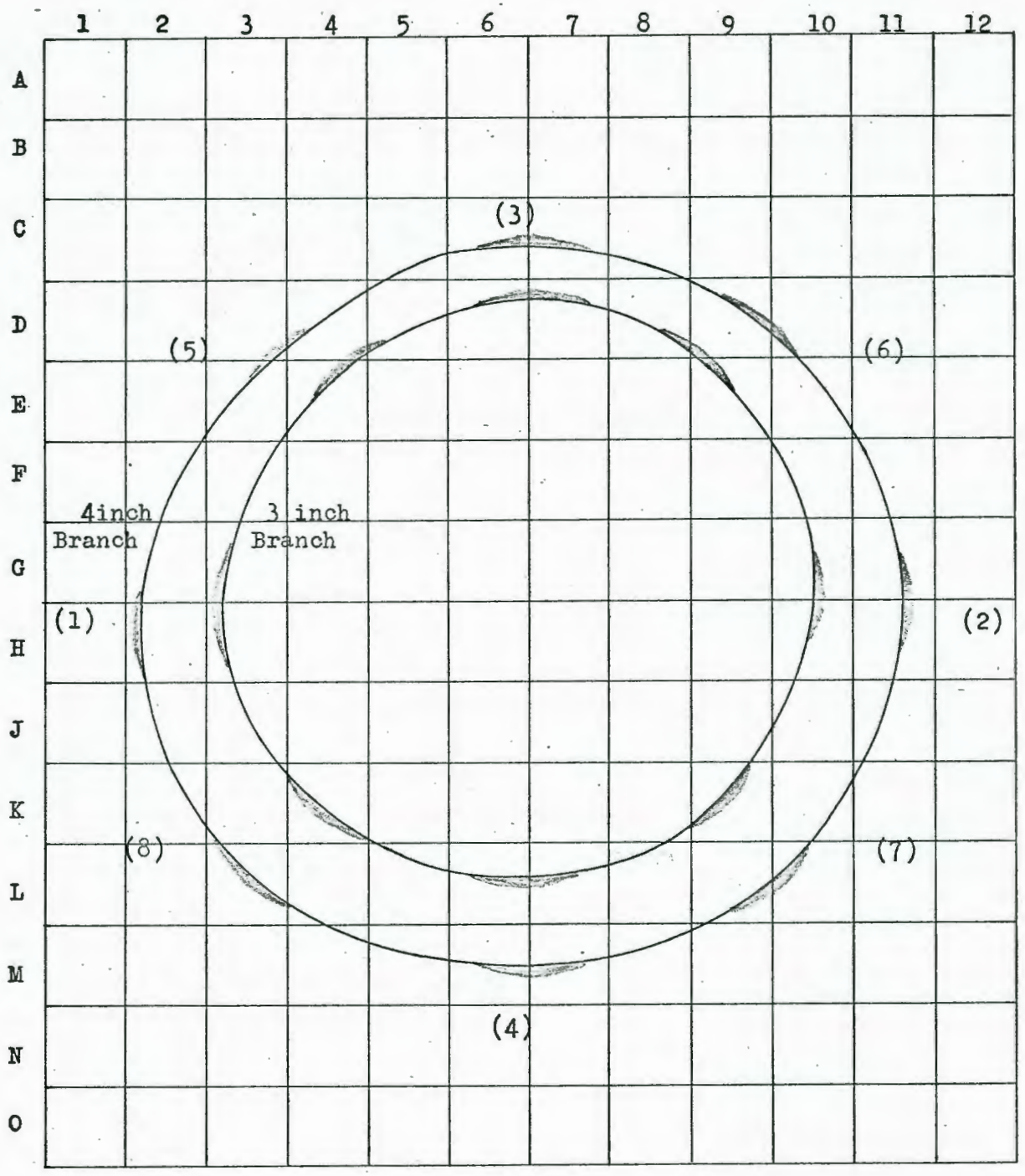

FIGURE VIII

CONNECTION OUTLINE AND AREAS OF INVESTIGATION

MODELS WITH $\phi = 45^{\circ}$

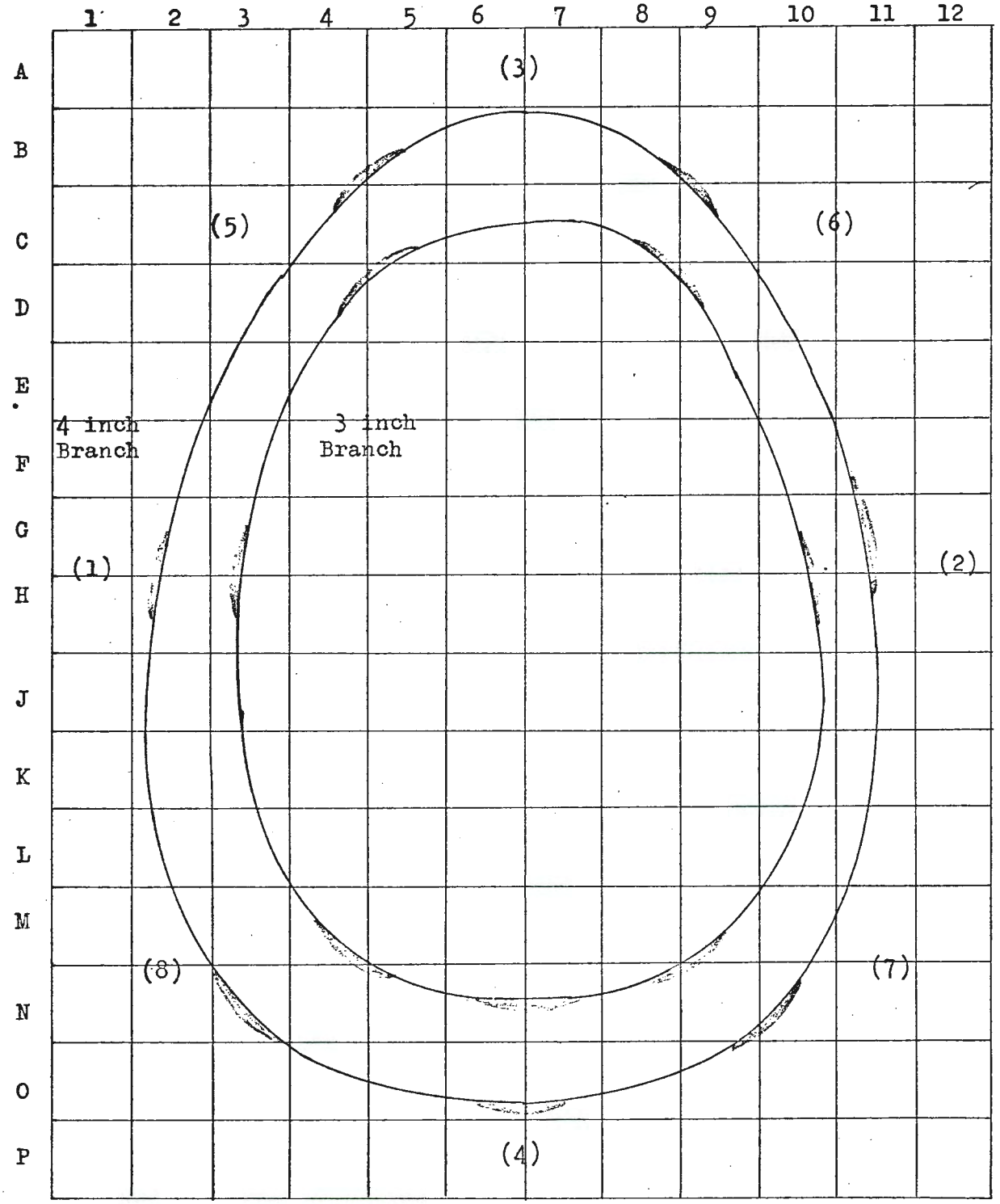

FIGURE IX

PHOTOELASTIC PLASTIC COATING - THICKNESS CONTOURS

CORD WITH BRANCHES AT $\phi = 90^{\circ}$

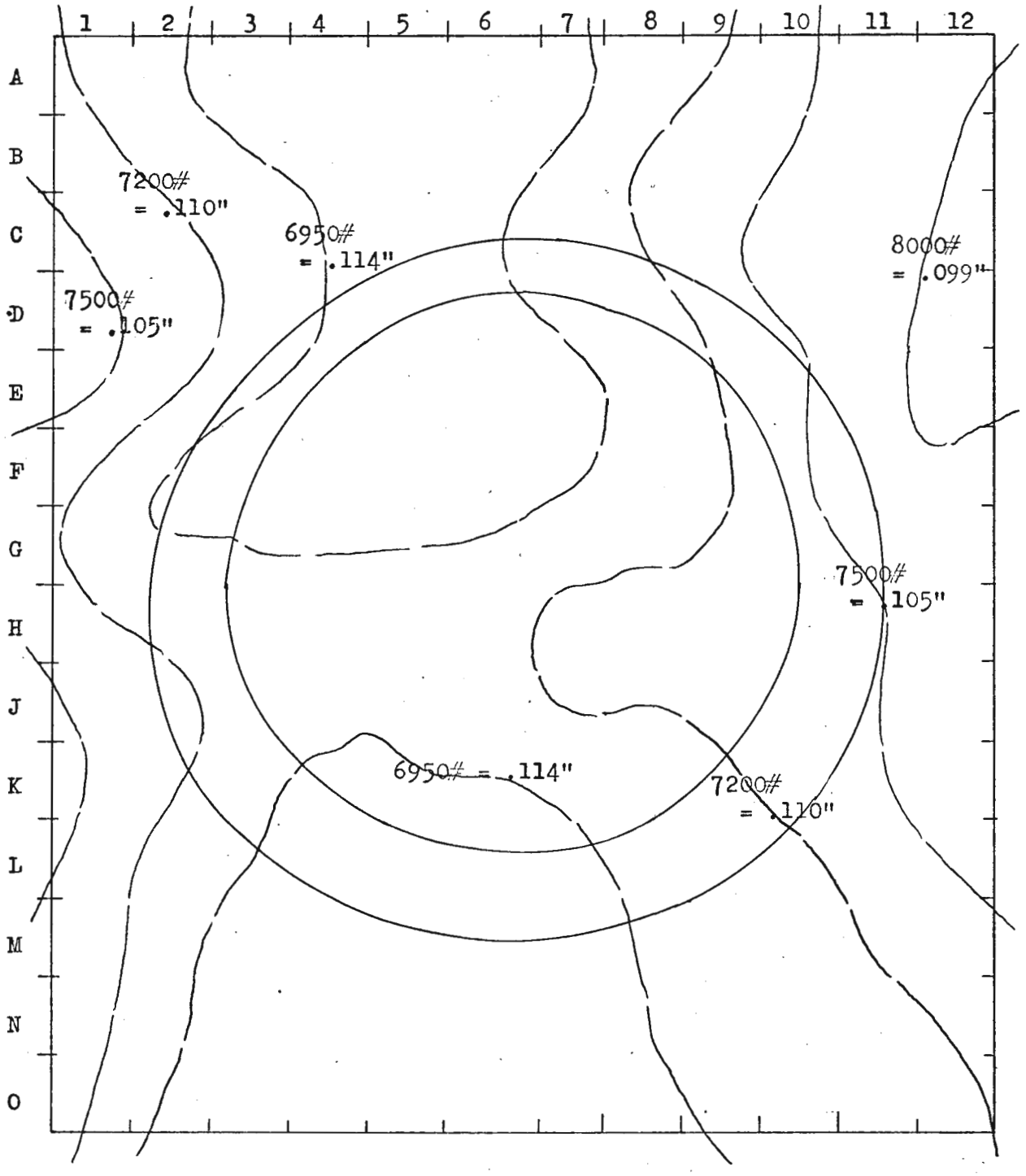

FIGURE X

PHOTOELASTIC PLASTIC COATING - THICKNESS CONTOURS

CORD WITH BRANCHES AT $\phi = 45^{\circ}$

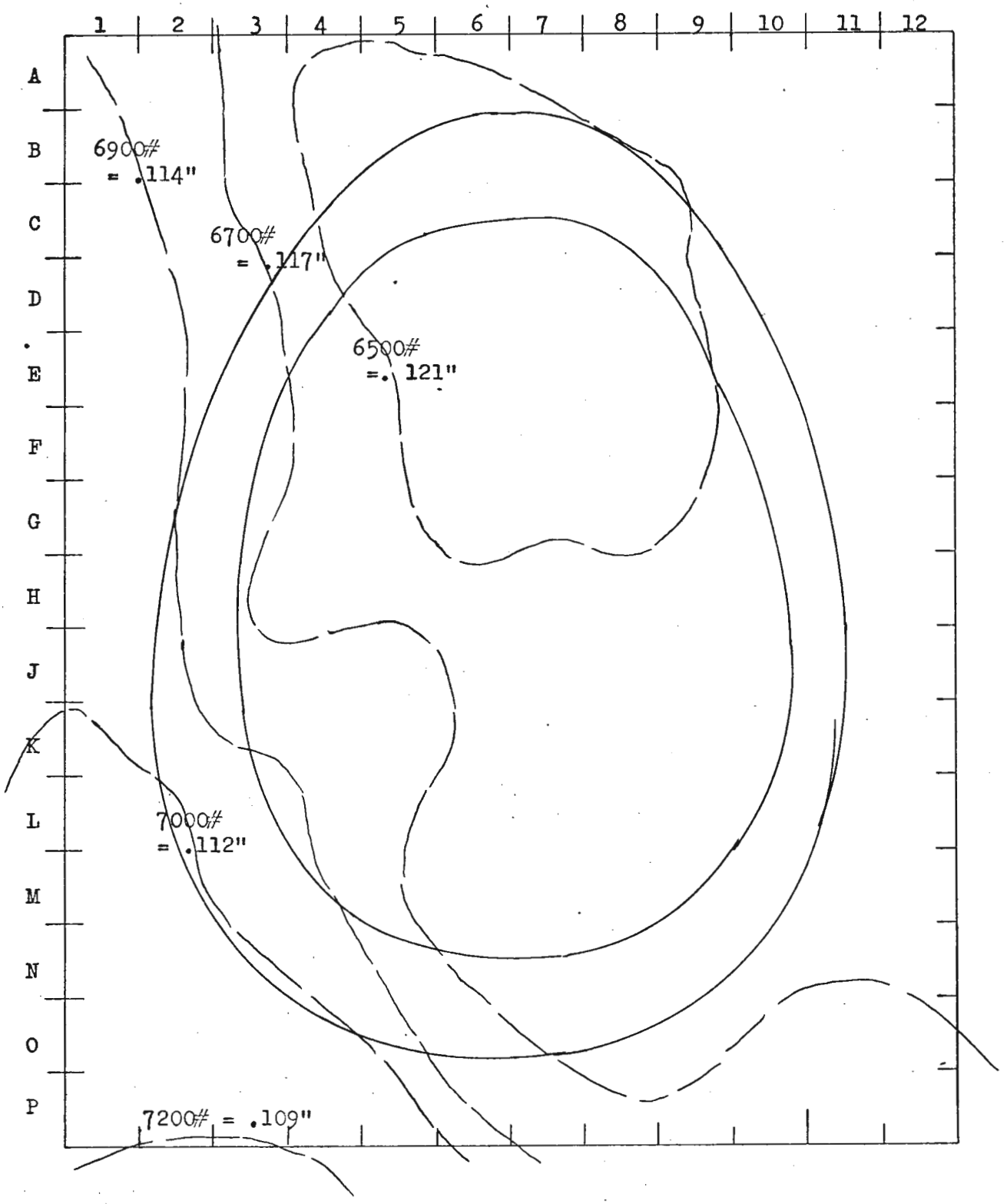

FIGURE XI

CASTING APPARRATUS AND CONTOURING PROCEDURE

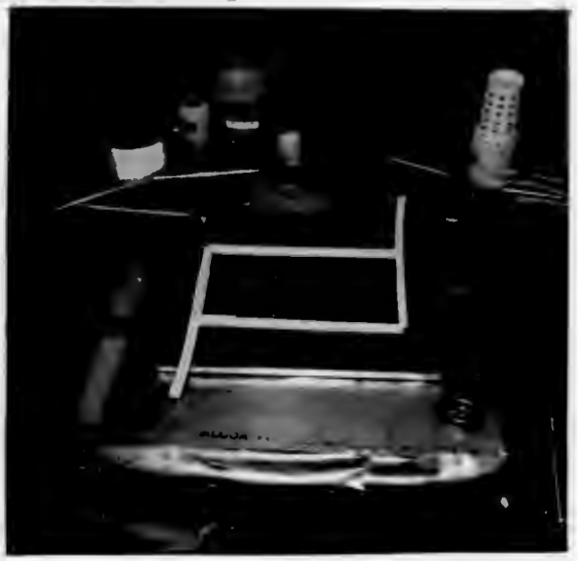

FIGURE XII

MODEL SETUP FOR TEST IN INSTRON

RESULTS

The results are presented as plots of branch load L vs Cord load F for each of the models tested. These plots consist of lines of constant principal stress difference or constant shear strain for various points within the area of investigation as shown in Figure IV . The points represent data taken from the model tests with dashed lines showing their trends. The solid lines represent predictions by mathematical means of the first fringe.

Prior to these plots a table of the effect of the application of the branch to the cord is presented. It will be noted that some areas experienced a reinforcing effect while others experienced stress concentrations.

TABLE I

FACTORS OF STRESS CONCENTRATIONS FOR $\phi = 45^{\circ}$ BRANCH

Branch Size (inches)	Area	Location	t_p (inches)	Predicted* 1st fringe at F = (Pounds)	Actual 1st fringe at F = (Pounds)	Factor = Predicted / Actual
3	(1)	GH-3	.117	6752	8300	0.81
	(2)	GH-9	.119	6613	8300	0.80
	(3)					
	(4)					
	(5)	CD-45	.121	6514	6250	1.04
	(6)	CD-89	.121	6514	6250	1.04
	(7)	MN-89	.118	6673	6250	1.07
	(8)	MN-45	.114	6910	6250	1.10
4	(1)	GH-2	.114	6910	8350	0.83
	(2)	FGH-11	.119	6613	7750	0.85
	(3)					
	(4)	O-67	.116	6791	7850	0.87
	(5)	BC-45	.121	6514	5500	1.18
	(6)	BC-89	.121	6514	5500	1.18
	(7)	N-910	.117	6752	6200	1.09
	(8)	N-3	.112	7029	6200	1.13

* This predicted first fringe is the same as if no branch were applied.

TABLE II

FACTORS OF STRESS CONCENTRATIONS FOR $\phi = 90^{\circ}$ Branch

Branch Size (inches)	Area	Location	t_p (inches)	Predicted 1st fringe at F = (Pounds)	Actual 1st fringe at F= (Pounds)	Factor = Predicted / Actual
3	(1)	GH-3	.113	6970	8000	0.87
	(2)	GH-10	.107	7366	8000	0.92
	(3)	D-67	.114	6910	7100	0.97
	(4)	L-67	.114	6910	7100	0.97
	(5)	DE-4	.114	6910	5250	1.32
	(6)	DE-89	.111	7108	5250	1.35
	(7)	K-9	.111	7108	5250	1.35
	(8)	K-4	.113	6970	5250	1.33
4	(1)	H-2	.112	7029	8050	0.87
	(2)	GH-11	.105	7504	8250	0.91
	(3)	C-67	.114	6910	7400	0.93
	(4)	M-67	.114	6910	7000	0.99
	(5)	D-3	.113	6970	5000	1.39
	(6)	D-910	.106	7425	5600	1.33
	(7)	L-910	.111	7108	5450	1.31
	(8)	L-3	.114	6910	5150	1.34

FIGURE XIII

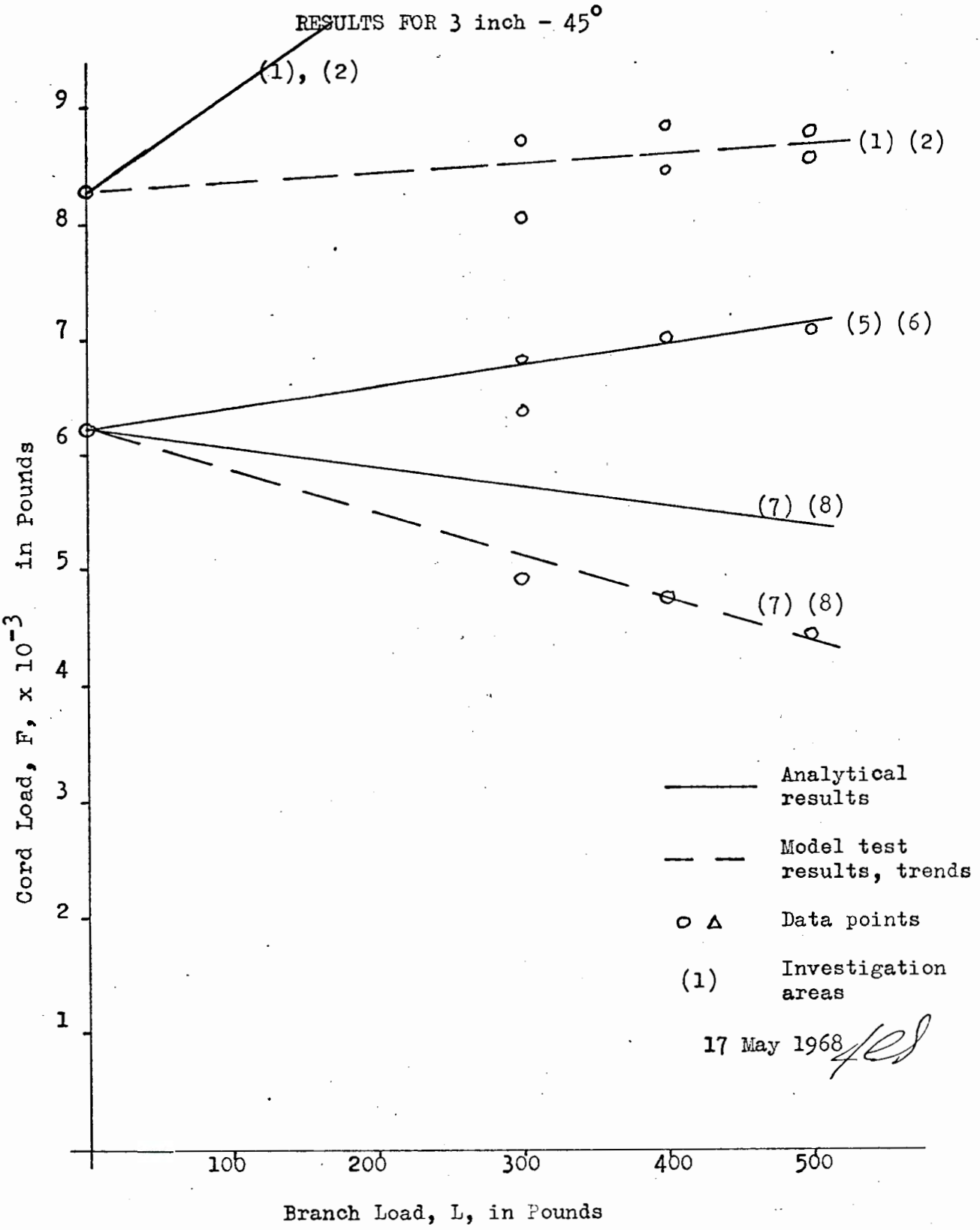
RESULTS FOR 3 inch - 45°
(1), (2)
(1) (2)
(5) (6)
(7) (8)
(7) (8)
9
8
7
6
5
4
3
2
1
Cord Load, F, x 10⁻³ in Pounds
100
200
300
400
500
Branch Load, L, in Pounds
Analytical results
Model test results, trends
Data points
(1) Investigation areas
17 May 1968

FIGURE XIV

RESULTS FOR 4 inch - 45°

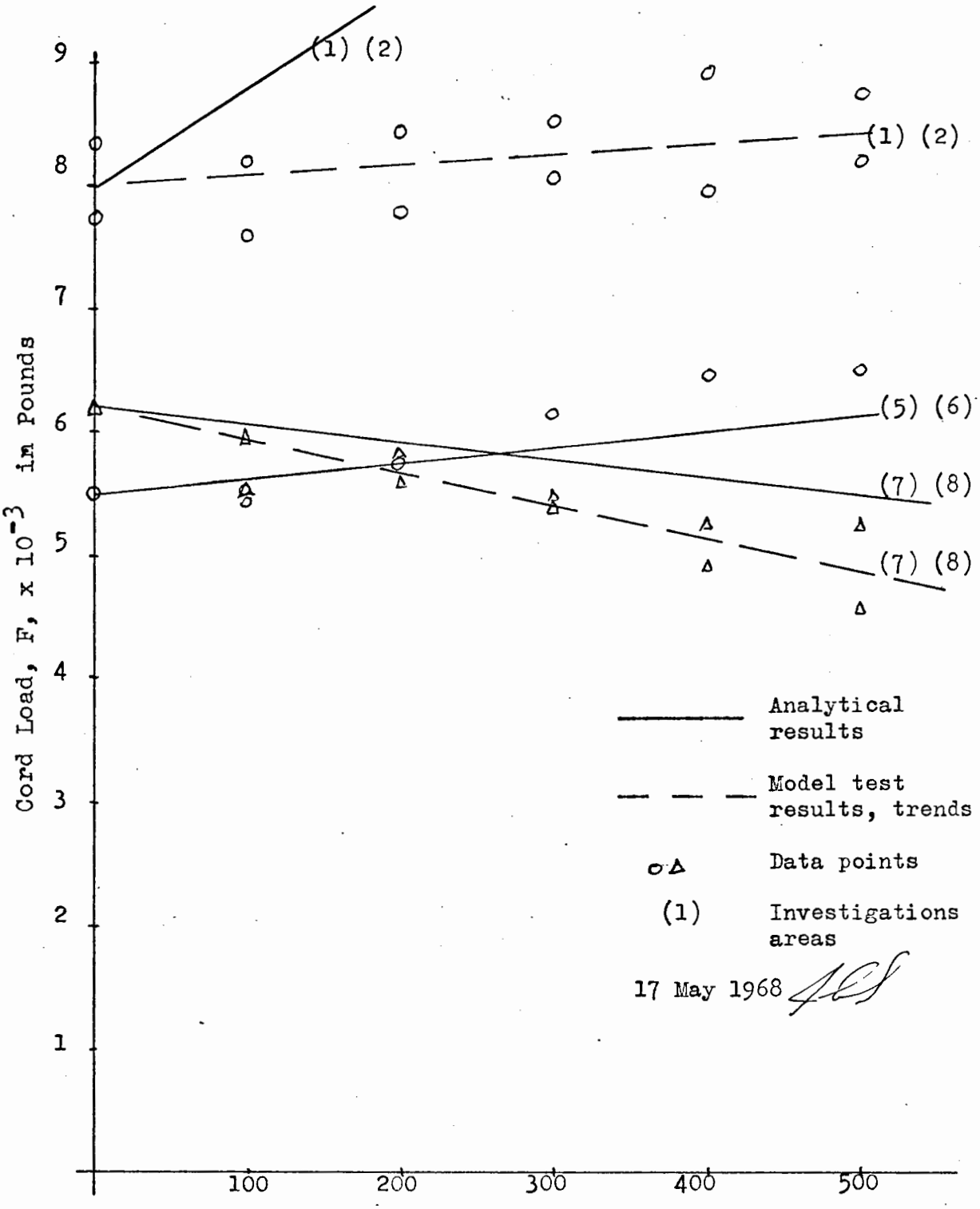

FIGURE XV

RESULTS FOR 3 inch - 90°

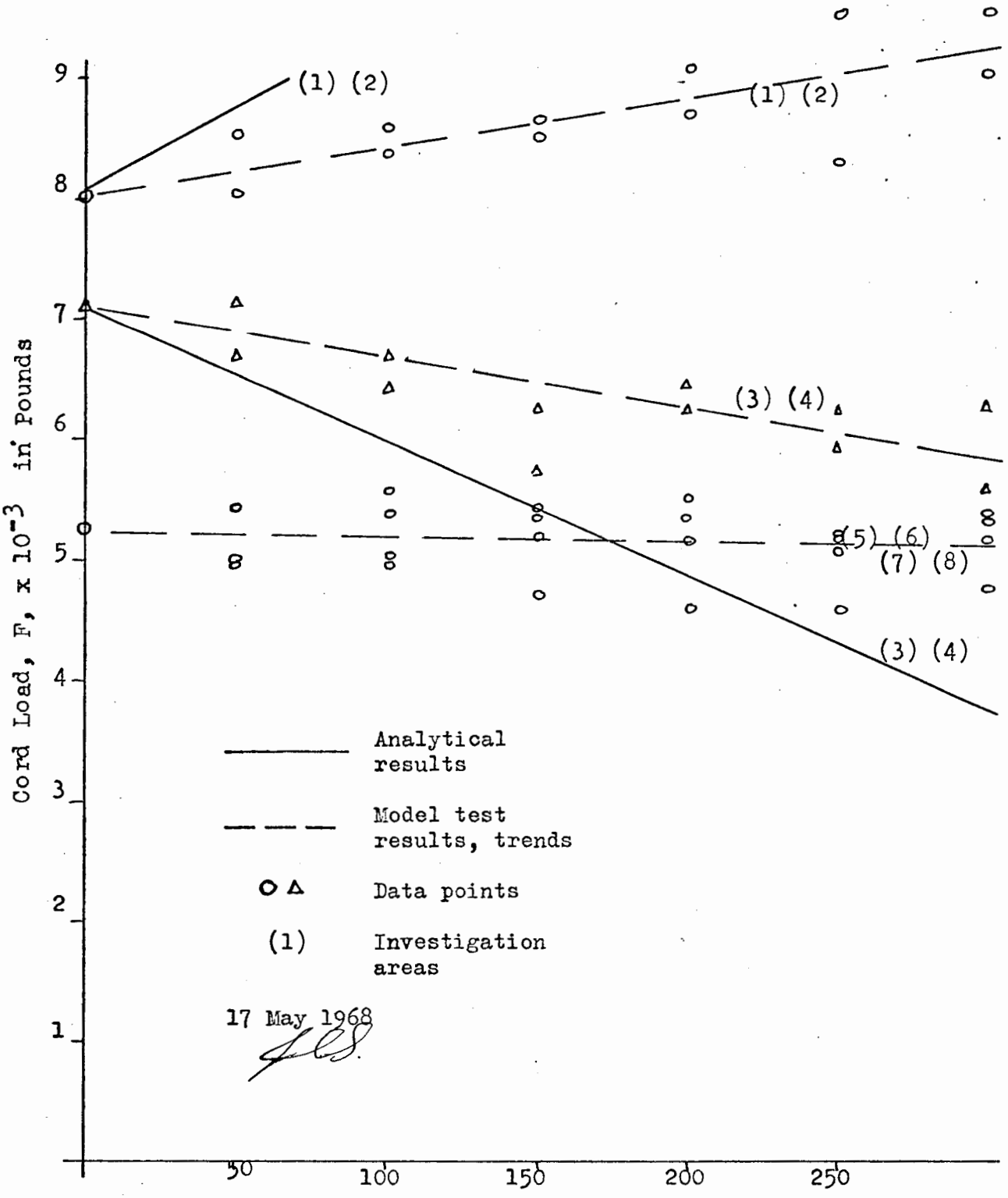

FIGURE XVI

RESULTS FOR 4 inch - 90°

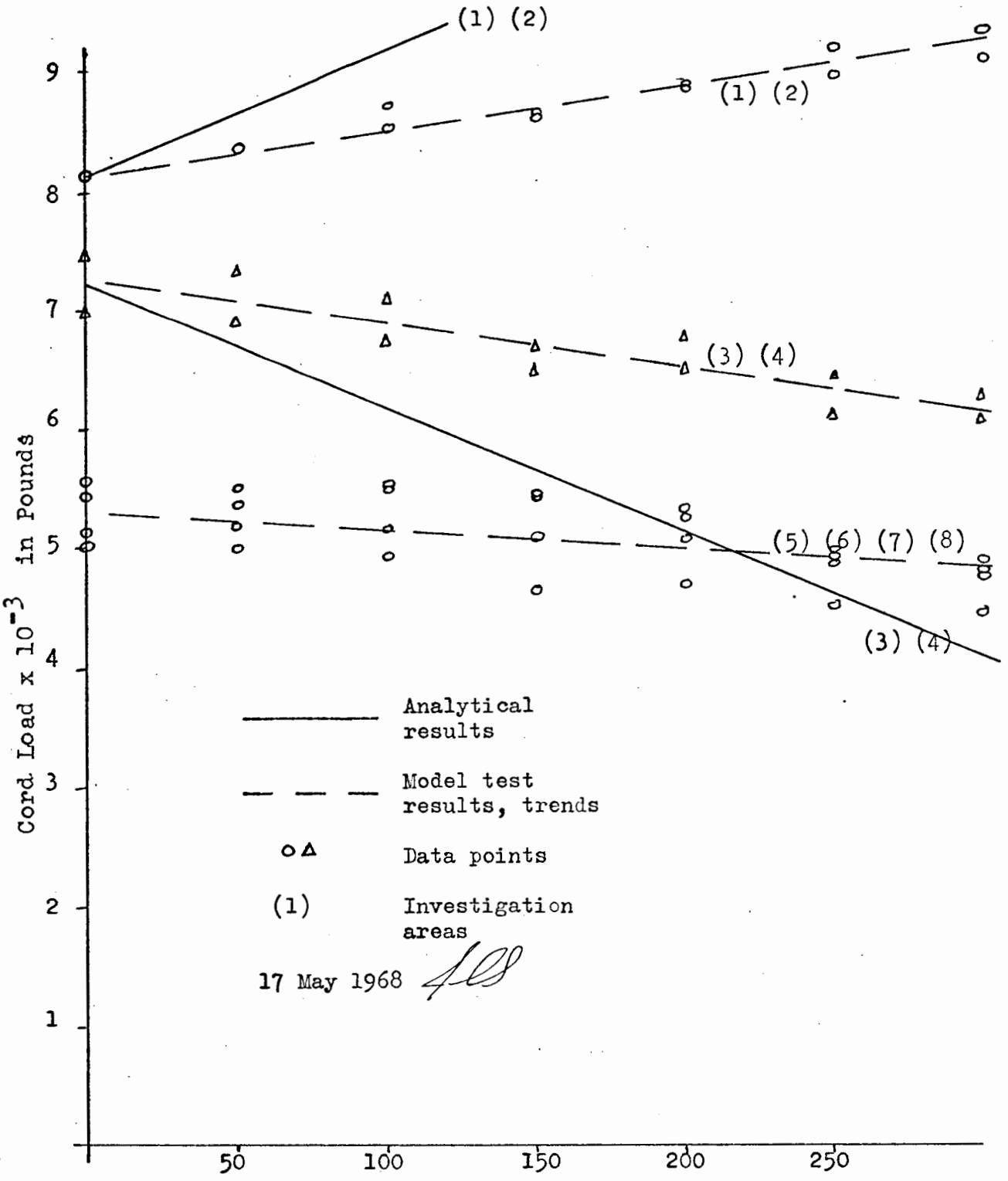

DISCUSSION OF RESULTS

The finding of the effect of the application of the branch was the first item in preparation of the results. This was necessary to insure that all plots were on a common basis. The analytical results from Hovgaard's Analysis or the Column Analogy of course did not have any effect of interaction between the cord and branch. The data for determining these effects was gathered from the model tests. The models were loaded with pure axial load prior to the application of the branch to observe the resulting fringe pattern and determine thickness contours as shown in Figures IX and X. Then branches were then applied and the pure axial cord loading was repeated to observe the appearences of the first fringe in the cord at the connection. The load which produced to fringe at various locations was recorded and the factor was figured as the load to produce first fringe without the branch, divided by the load to produce the first fringe with the branch applied.

The next step in preparing the results was to determine by the analytical means mentioned above the stresses in the cord from the branch load. These methods are described in the appendix and sample calculations presented there. The results were a moment M and circumferential force H at areas (1) and (2) acting in the circumferential direction and were in terms of L, the branch load. In the analyses, the load which was taken to produce this moment and force was the total branch load L divided into two point loads acting at a distance equal to the branch radius. In the case of the 45° branch models, the moment and force were reduced by .707 to account for the fact that the branch was treated as two loads, one acting perpendicular to the cord centerline and the other acting as a shearing force V on the face of the cord. These forces, M, H and V were translated

into stresses and combined with the axial stress from the cord load F, by Mohr's circle to determine the value of the difference in principal stress or maximum shear stress. The resulting equation (26) in terms of L and F was solved for F with a predetermined value of $S_1 - S_2$ and by choosing a value of L. The value of $S_1 - S_2$ was that which theoretically would produce a frimge at area (1) or (2). The line thus produced is shifted to account for the stiffening effect of the branch.

As soon as the first analytical results were plotted against the model test data, it was very evident that the analysis was producing F loads far in excess of that which was actually needed for the appearence of the first fringe. It was necessary therefore to modify the analyses and use smaller loads. A load per circumference, L/C_b , proved to give much closer results even though still predicting a higher F than the model tests.

The prediction of the appearence of fringes at other locations, could not be done with Hovgaard's Analysis or the Column Analogy, for these analyses only treated the areas (1) and (2). The plotted model data helped in the attempt at this prediction, which correlated well in some areas and rather poorly in others.

The plot of the model test results, showed that in the case of the 90° branch, the areas (5) (6) (7) and (8) showed almost no effect from the varying of the branch load. This suggested that the maximum shear stress at these points remained constant. Whether the principal stresses changed or remained constant, their difference did remain contant. This lead to the idea that in the case of ϕ being other than 90°, the prediction of the stress for the above mentioned areas could be accomplished by taking the shear component V, of the branch load

alone, and combining this as tension or compression to the axial stress S_f from the cord load F.

The combining of stress to predict the stress in areas (3) and (4) did not produce as good results as did the other predictions. The method used was to take the moment M alone as predicted by Hovgaard's analysis, and combine this with the axial load. The stress used were .639 L and .610 L for the 3 inch 90°, .470 L and .476 L for the 4 inch 90° branches. The plot of the model data on the other hand, suggested that the stress from the branch, S_b, provided there was no shear stress present, should have been of the order of 0.19 L.

CONCLUSIONS

1. This thesis only looked at the surface stress and was unable to establish any trends of the stress through the wall of the cord.

2. The circumferential force H, from the branch-load contributed only about 1 % to the total stress from the branch and therefore may be considered negligible.

3. Hovgaard's Analysis and the Column Analogy predicted a moment from the branch load much too high, even when the load producing this moment was taken as the branch load divided by the circumference of the branch, L/C_b. The predicted S_b was found to be 2.5 to 3.2 higher than the model tests showen, for the appearance of the first fringe and areas (1) and (2).

4. Areas (5), (6), (7), and (8) can be predicted with a fair accuracy by taking the shear component of the branch load as the only load, besides the cord load F, that effects the value of the maximum shear stress or $S_1 - S_2$. It is postulated that the moment component of the branch load produces stresses of equal magitude in the axial and circumferential directions, thereby having no effect on the fringe pattern or appearance at these points.

5. The moments applied to the end of the cords in the model tests were not treated in these results. The additional normal and shear stress introduced by an end moment can be easly determined for the case where are no discontinuities, as the cord without the branch. With the addition of the branch , whether loaded or not, the resulting shear and stress distribution or pattern, from these end moments, would only have complicated the results to the point where this paper may not have produced any acceptable results or conclusions.

RECOMMENDATIONS

A very small start was attempted in this thesis to discover what is happening in the area surrounding the cylindrical joint with a continuous cord. A great deal more investigation must be done with this type of joint before a clear understanding of what is happening within either the cord or the branch will be known.

Some of the possible further studies are listed below. They consist of two basic areas. The method of investigation may be accomplished by either, brittle coadings, strain gages, photoelastic coating, or by photoelastic stress freezing methods.

1. The effect on the cord of the application of a branch. The stress pattern and distribution, in both the cord and the branch when the cord is subjected to axial loads and moments, but no branch load. This should consist of varying cord loads, moments and branch size to determine stress concentration and their locations. This type of study would give the basic understanding of how the branch effects the cord.

2. The distribution of branch load into the cord. Here the actual distribution of the branch load as forces, moments and shears within the cord. This distribution should be found not only at the connection but around the circumference of the cord as well in order to form some analytical method for determining these forces, moments and shears.

If these studies are carried out by some surface method such as brittle coatings, strain gages, or photoelastic coatings. Their results could further be checked by a photoelastic stress freezing analysis and at the same time obtain the distribution of stresses through the wall of the branch and cord.

APPENDIX

NOTATIONS

A = area of analogous column (Column Analogy)

= 24a

a = member area (Column Analogy)

= lt

A_b = Branch cross sectional area

A_c = Cord cross sectional area

c = distance from neutral axis

C_b = circumference of cord

C_c = circumference of branch

E = modulus of elasticity of plastic

= 420,000 p.s.i.

e = amount of eccentricity of cord load F

F = cord axial load

H = circumferencal force in Hovgaard's Analysis which is uniform through the thickness. a compressive force being positive.

H_i = the component of a load centerline reaction, on the cord between station 0 and the point in question, which is acting in the same direction as the tangent to the cord at this point. (Hovgaard's Analysis)

H_o = H force acting on station 0 (Hovgaard's Analysis)

I = moment of inertia of cord wall about its neutral axis in the circumferencal direction.

I_c = moment of inertia of the cord about its centerline.

I_x and I_y = moment of inertia of analogous column (Column Analogy)

$= \pi t r_c^3$

K = fringe constant for photoelastic plastic

$= S_1 - S_2 \; / \; n/t_p$

L = component of branch load perendicular to cord centerline

l = member length of analogous column (Column Analogy)

M = total moment acting at a section in either Column Analogy or Hovgaard's Analysis.

M_B = bending moment at a station produced by external loads (Hovgaard's Analysis)

m_i = fiber stress (Column Analogy)

m_s = moment at any section produced by the loads acting on the structure if cut in any way so that it is statically determinate (Column Analogy)

M_x = monent of the load along the x axis about y axis (Column Analogy)

M_y = monent of the load along the y axis about x axis (Column Analogy)

M_0 = moment at station 0 in (Hovgaard's Analysis)

n = fringe order

P = axial load (Column Analogy)

$= \sum m_s a$

r_b = radius to mid-thickness of branch

3 inch branch = 1.635 inches

4 inch branch = 2.105 inches

r_c = radius to mid-thickness of cord

= 4.21 inches

R_1 and R_2 = assumed Reactions to branch load used in Hovgaard's Analysis and Column Analogy to satisfy static equilibrum.

S = stress

s = strain

S_b = stress in cord from component of branch load perpendicular to cord centerline.

s_b = strain in cord from component of branch load perpendicular to cord centerline.

S_f = stress in cord from end loads on cord.

s_f = strain in cord from end loads on cord.

S.M. = Simpson's Multipilier

S_1 and S_2 = principle stress

T = shear stress in cord

t = wall thickness of the cord including pipe and photoelastic plastic.

$= t_p + t_c$

t' = thickness of analogous column numerically equal to 1/EI

t_b = pipe wall thickness of branch

t_c = pipe wall thickness of cord

t_p = photoelastic plastic thickness

T_v = shear stress in cord due to component of branch load parallel to the cord centerline.

V = shear loading from branch or component of branch load parallel to cord centerline.

v = Poisson's Ratio for the plastic. Both pipe and photoelastic

ν con't. coating had the same value.

$= 0.36$

$\bar{x}$ and $\bar{y}$ = coordinates axis system with origin at station zero (Hovgaard's Analysis)

x_o and y_o = coordinates axis system with origin at centerline of cord or analogous column (Column Analogy)

θ = angle giving location of a point around the circumference of the cord measured from the positive x_o axis with positive direction being counterclock wise.

$\bar{\theta}$ = angle between positive $\bar{x}$ axis and a tangent to the cord.

$= 90^o + \theta$

ϕ = angle between cord centerline and branch centerline.

DETAILS OF PROCEEDURE

PHOTOELASTIC PLASTIC COATING

The plastic chosen for this work was a high modulus liquid plastic, Photolastic Incorporated's PL-1, with a modulus elasticity of approximately 420,000 p.s.i. This most closely mached the pipe used, Barrett PVC TD-3, which exhibites an average modulus of also 420,000 p.s.i.

The casting of the plastic coatings was accomplished after three attempts due to difficulties with the casting plate. The first attempt was made with a glass plate covered with a teflon coated heavy aluminum foil for a non-adherence medium between the liquid plastic and the glass. This proved unsatisfactory because of the glass being a poor conductor of heat, causing the liquid to cool unevenly. The second attempt was made with a heavy aluminum slab, sanded smooth and liberally coated with a silicon releasing agent. This also proved unsatisfactory because of adherence of the liquid plastic to the aluminum plate inspite of the releasing agent. The third attempt was successful. The teflon coated aluminum foil was removed from the glass plate and reapplied to the aluminum slab. This combined the good heat conduction properties of the aluminum slab with the releasing properties of the teflon.

The actual casting of the sheets of plastic were accomplished by the process given in Reference 24 , and the cementing process was according to Reference 26 . Several comments on the casting and cementing process were noted.

Casting Process

1. After the sheets were cast it was noted that the casting plate was not perfectly flat. This caused a gradual variation of plastic thickness from one point to another. This effect was not harmfull for it

was taken into account later.

2. When the teflon coated aluminum foil was removed, some rinkles and creases resulted, all of which would not be removed prior to reapplication. This did prove harmfull as explainded below.

3. If the releasing agent is not applied very carefully it has a tendency to form droplets rather than a uniform liquid layer. This also proved harmfull.

The difficulties described in paragraph 2. and 3. above, came when the thickness of the coating was attempted to be measured. The ridges and rinkles in the teflon-aluminum foil and the beading of the releasing agent caused one side of the sheets to have a great many small hollows and valleys. Because the sheets were curved to the contour of the cord, a regular micrometer could not be used for thickness measurements. The standard micrometer would have had a tendency to average out these effects. In stead a ball micrometer was used and the readings on thickness reflected the above mentioned variations.

4. It was also noted that the sheets must be handled very carefully in the contouring stage. It was found that very little pressure, even over a short period of time, would modify the thickness of the sheets.

The method used to compensate for the above mentioned thickness variation was to load the models, prior to application of the branches and observe the resulting stress pattern. The load was applied with zero eccentricity to produce a uniform stress through the coating. By sketching the fringe pattern at various loads, see Figure IX and X, thickness contours of the coating were determined. Attention was paid to the general pattern of the fringe and not to specific points, thereby disregarding the unwanted

varience in thickness. All through the model tests the general appearence of fringe was sought, not point appearences.

Cementing Process

The procedure followed proved to be a good process with the following notes. First one should not attempt to apply too many pieces of plastic with the same batch of cement. Within only a few minutes, the cement begins to become rather viscus. This makes application of the cement difficult as well as removal of any air bubles from between the plastic and cement. Secondly as an additional suggestion, cover the top surface of the plastic coating with polyvinyl sheeting and scotch tape the sheeting into place. This, along with the covering of the non-coated areas of the model as described in Reference 26, keeps the cement off unwanted areas and helpes to achieve neater model appearence. The tape should run along the very edge, on the top of the plastic, to provide a good sharp glue line. Although masking tape is easer to apply and remove, it should not be used. Being non-transparent, the masking tape could allow bubbles to be left between the plastic and cement in this area.

MODEL TESTING PROCEEDURE

The models were tested in a Instron machine providing a maximun compressive force to the cord of 20,000 pounds. The cords were loaded both in pure axial compression and axial compression with end moments. The moments were supplied by known amounts of eccentricity of the end loads.

The branch load was supplied by means of wire cables putting the branchs in pure axial compression. With the branches applied, test runs were made holding the branch load constant and increasing the cord load. Readings on the branch load, cord load and eccentricity, were taken at

the appearence of fringes in certain locations. These locations were generally at the following places in the cord; the top, bottom and sides of the cord-branch intersection, and the regions 45° on either side of the plane joining the centerlines of the cord and branch at the cord-branch intersection. All data was taken in pounds of force and inch-pounds of force and inch-pounds of moment.

Prior to the molding process, test strips were cut from the plastic sheets and cemented to steel bars. This process was for the determination of the fringe constant K of the photoelastic plastic. The bars were subjected to a known amount of strain and the number of fringes thus developed in the plastic read. Since strain is linear through the composite bar, steel with plastic coating, a correction was make for the thickness of the plastic. The plastic was applied to both sides of the bar negating any shift in the neutral axis, but being of relatively low modulus and fairly thin the plastic was considered to have no reinforcing effect on the steel. The strain at the surface of the steel was 1700 micro inches / inch and the strain at mid-thickness of the plastic was

$$s_1 - s_2 = 1700\,(1 + v_m)\left(\frac{.120 + .006 + .045}{.120}\right) \qquad (1)$$

$$= 3120 \text{ micro inches/ inch}$$

where

v_m = Poisson's ratio for the steel

.120 = $\frac{1}{2}$ steel thickness

.006 = cement thickness

.045 = $\frac{1}{2}$ plastic thickness

the fringe constant in terms of strain

$$K\ (\text{strain}) = \frac{s_1 - s_2}{n \,/\, t_p} \qquad (2)$$

$$= \frac{3120}{2.167}\ (.090)$$

$$= 129 \text{ micro inches/inch/fring/inch}$$

where

2.167 = number of fringes observed

and the fringe constant K in terms of stress

$$K = \frac{s_1 - s_2}{n/t_p}\left(\frac{E}{1+v}\right) = \frac{S_1 - S_2}{n/t_p} \qquad (3)$$

$$= 129 \times 10^{-6}\left(\frac{420{,}000}{1+.36}\right)$$

$$= 39.8 \text{ p.s.i./fringe/inch}$$

This value for K was used throughout the investigation.

FIGURE XVII

MEMBER OR STATION LOCATIONS AND COORDINATE SYSTEMS

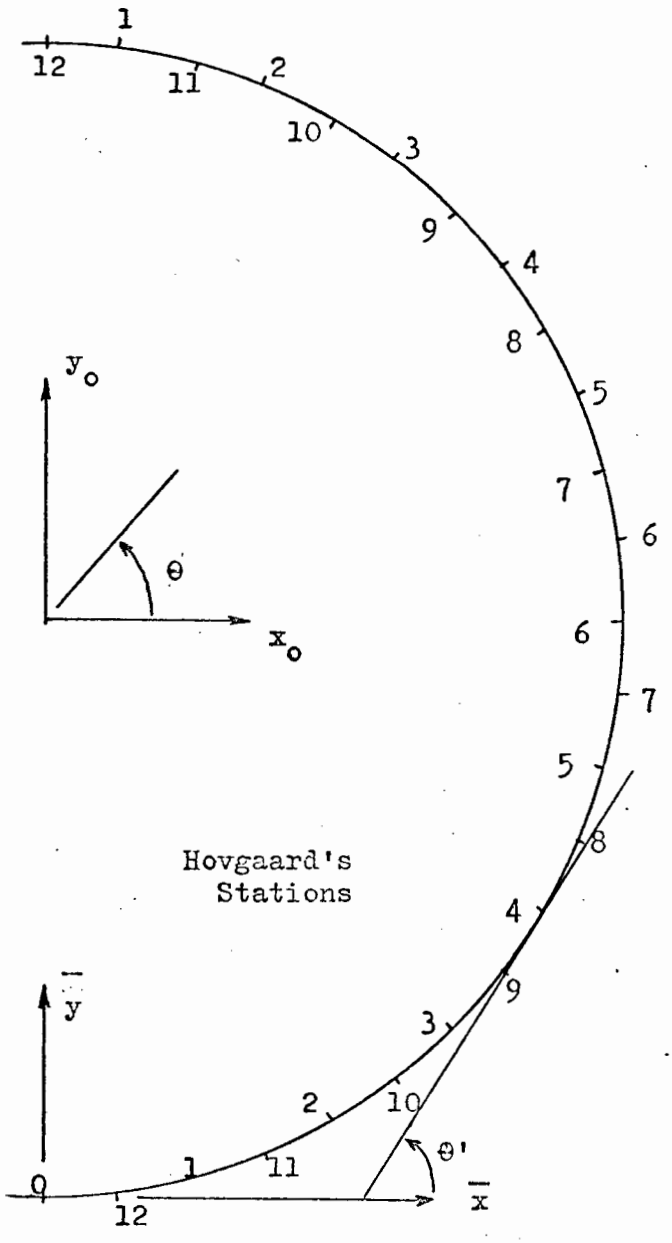

MATHEMATICAL ANALYSES

Analysis was done by both Hovgaard's Ring Frame Analyses [3], and Hardy Cross's Column Analogy [18]. A series of analyses were done with both methods, using as a variable the position of the reactions. The branch load was left in terms of L for all analyses. The reactions R_1 and R_2 satisfy equilibrium for the two dimensional analogy of the cylindrical joint. Both Hovgaard's Ring Frame Analyses and Hardy Cross's Column Analogy produce a moment distribution around the circumference of the cord which satisfies continuity. The moment resulting from these analysis at the connection of the cord and branch, was used to determine the circumferential stress in the cord due to the branch load at the connection.

In the following analyses all forces are in terms of pounds and moments are in terms of inch-pounds. In both Hovgaard's Analyses and Column Analogy those moments which produce tension on the inside fibers of the cord carry a positive sign. In the tabulated results of these analyses the "analysis number", referes to the location of the reactions as given in Table III.

COLUMN ANALOGY

The Column Analogy arises from the fact that a frame subjected to in plane loads exhibits the same form of equations for displacement and rotation of a point as an analogous column of the same shape, with thickness of 1/EI*, subjected to axial loadings. See Reference [11] for complete

---

* Where the E and I refer to the frame not the analogous column.

TABLE III

TABLE OF REACTION LOCATIONS

Analysis Number*	Reaction R_1		Reaction R_1	
	Location**	x	Location**	x
1	***	3.28	***	3.28
2	9	2.98	4	3.65
3	9	2.98	5	4.07
4	9	2.98	6	4.21
5	8	3.65	5	4.07
6	8	3.65	4	3.65
7	8	3.65	3	2.98
8	7	4.07	5	4.07
9	7	4.07	4	3.65
10	7	4.07	3	2.98
11	6****	4.21	6****	4.21
12	6	4.21	6	4.21

* These analysis numbers and their corresponding reaction locations are commonly used in both Hovgaard's Analysis and Column Analogy.

** Refers to Hovgaard's stations as shown in Figure XVII.

*** This location was determined by placing the reactions at twice the x distance of the 3 inch branch load L/2.

**** This location was determined by placing reactions at twice the x distance of the 4 inch branch load L/2 which placed both R_1 and R_2 at station number 6.

discription of this analyses.

The cord was divided into 24 stations spaced at 15° apart as shown in Figure XVII. Analysis was carried out in tabular form based on the following formulas:

$$I_x = I_y = \pi t r_c^3 \tag{4}$$

$$= \frac{203}{EI}$$

$$l = 15^{\circ} \left(\frac{\pi}{180}\right) r_c \tag{5}$$

$$= 1.102 \text{ inches}$$

$$a = lt \tag{6}$$

$$= \frac{1.102}{EI}$$

$$A = 24\ a \tag{7}$$

$$\sum m_s a = P \tag{8}$$

$$\frac{P}{A} = \frac{\sum m_s a}{24a} = \frac{\sum m_s}{24} \tag{9}$$

$$m_y = m_s\ a\ y_o \tag{10}$$

$$\sum m_y = M_y \tag{11}$$

$$m_i = \frac{P}{A} + \frac{M_x}{I_x} x_o + \frac{M_y}{I_y} y_o \tag{12}$$

but because of the cord being symetrical about the y_o axis

$$M_x = 0$$

therefore

$$m_i = \frac{P}{A} + \frac{M_y}{I_y} y_o$$

and the total moment at any station

$$M = m_s - m_i \tag{13}$$

Almost all of the above calculations were done in tabular form, see tables IV and VI.

The results from these analyses were tabulated in tables V and VII . Figures XVIII & XIX show the distribution of M around the cord. The moments are plotted radially from the cord with positive being inward. The plot shows a band of M which contains all the analyses moment curves.

HOVGAARD'S ANALYSIS

Hovgaard's Contineous Ring Frame Analysis has long been used in structural design of ships and its tabular method for satisfing continuity is familiar to most naval architects. Here its method was extended in an attempt to predict the stress in a cylinderical joint.

Complete discussion of this analysis is carried in Hovgaard's book Reference 3 . As in the Column Analogy the cord was divided into 24 stations starting with station 0 at the origin of the coordinate system, see Figure XVII. Besides the tabulation shown in Tables IX and XI , the basic equations for this analysis are:

$$\int \frac{M}{E\,I}\,ds = \frac{1}{E\,I}\int M ds = 0 \tag{14}$$

$$\int y\,\frac{M}{E\,I}\,ds = \frac{1}{E\,I}\int yM ds = 0 \tag{15}$$

which become the following when applyed to definate intervals;

$$\Sigma\ (S.M.)\ M = \Sigma\ \left[(S.M.)\ M_o + y\ (S.M.)\ H_o + (S.M.)\ M_B\right] = 0 \tag{16}$$

$$\Sigma\ y\ (S.M.)\ M = \Sigma\ \left[y\ (S.M.)\ M_o + y^2\ (S.M.)\ H_o + (S.M.)\ M_B\right] = 0 \tag{17}$$

These two equations are solved simultaneously for M_o and H_o. Then the moment M at each equation is given by

$$M = M_o + yH_o + M_B \tag{18}$$

TABLE IV

3 INCH BRANCH COLUMN ANALOGY

ANALYSIS NUMBER 1

Member	x_o	y_o	m_s a	m_y	$\frac{M_y}{I_y} y_o$	m_i	M
1	0.55	4.18	0 La	0 La	+.3566 L	- .3609 L	+.361 L
2	1.60	3.91	0 La	0 La	+.3335 L	- .3840 L	+.384 L
3	2.55	3.35	- .455 La	-1.524 La	+.2858 L	- .4317 L	-.094 L
4	3.33	2.57	- .833 La	-2.140 La	+.2192 L	- .4983 L	-.334 L
5	3.89	1.62	- .973 La	-1.575 La	+.1382 L	- .5793 L	-.393 L
6	4.17	0.56	-1.043 La	- .584 La	+.0478 L	- .6697 L	-.373 L
7	4.17	-0.56	-1.043 La	+ .584 La	-.0478 L	- .7653 L	-.277 L
8	3.89	-1.62	- .973 La	+1.575 La	-.1382 L	- .8557 L	-.117 L
9	3.33	-2.57	- .833 La	+2.140 La	-.2192 L	- .9367 L	+.104 L
10	2.55	-3.35	- .820 La	+2.747 La	-.2858 L	-1.0033 L	+.183 L
11	1.60	-3.91	- .820 La	+3.206 La	-.3335 L	-1.0510 L	+.231 L
12	0.55	-4.18	- .820 La	+3.428 La	-.3566 L	-1.0741 L	+.254 L
			-8.610 La	+7.857 La			

$P = -17.22$ La $\qquad M_y = 15.714$ La

$\frac{P}{A} = -0.7175$ L $\qquad \frac{M_y}{I_y} = 0.0853$ L

TABLE V

3 INCH BRANCH COLUM ANALOGY

TABULATION OF ANALYSES RESULTS

Station	Moment M									
	Analysis Number									
	1	2	3	4	5	6	7	8	9	10
1	+.361L	+.328L	+.285L	+.281L	+.305L	+.339L	+.386L	+.303L	+.335L	+.382L
2	+.384L	+.353L	+.314L	+.306L	+.342L	+.369L	+.410L	+.342L	+.370L	+.411L
3	-.094L	-.053L	-.082L	-.086L	-.041L	-.023L	+.006L	-.031L	-.013L	+.017L
4	-.334L	-.286L	-.301L	-.301L	-.330L	-.325L	-.315L	-.307L	-.302L	-.292L
5	-.393L	-.340L	-.340L	-.335L	-.427L	-.438L	-.449L	-.448L	-.458L	-.471L
6	-.373L	-.315L	-.297L	-.286L	-.360L	-.388L	-.424L	-.408L	-.436L	-.473L
7	-.277L	-.215L	-.178L	-.171L	-.215L	-.262L	-.324L	-.244L	-.291L	-.353L
8	-.117L	-.050L	-.040L	-.049L	-.052L	-.072L	-.159L	-.064L	-.084L	-.171L
9	+.104L	+.101L	+.061L	+.057L	+.071L	+.095L	+.067L	+.075L	+.099L	+.158L
10	+.183L	+.183L	+.144L	+.144L	+.172L	+.183L	+.224L	+.189L	+.200L	+.241L
11	+.231L	+.231L	+.204L	+.207L	+.244L	+.246L	+.274L	+.271L	+.273L	+.301L
12	+.254L	+.257L	+.233L	+.232L	+.281L	+.277L	+.298L	+.311L	+.308L	+.330L

FIGURE XVIII

MOMENT DISTRIBUTION

Column Analogy - - 3 inchBranch

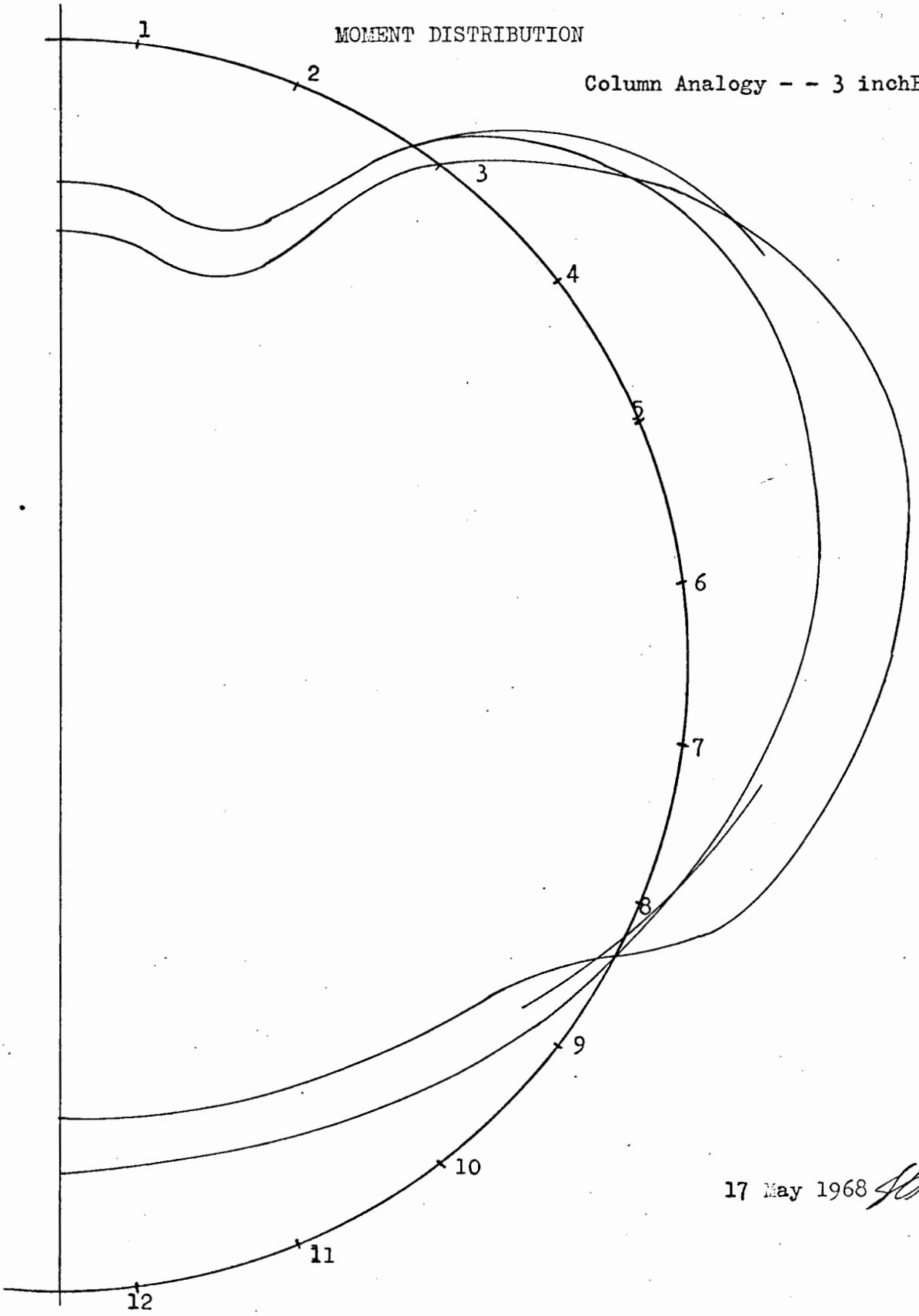

17 May 1968

TABLE VI

4 INCH BRANCH COLUMN ANALOGY

ANALYSIS NUMBER 10

Member	x_o	y_o	m_s a	m_y	$\frac{M_y}{I_y} y_o$	m_i	M
1	0.55	4.18	0 La	0 La	+.3595 L	-.2745 L	+.275 L
2	1.60	3.91	0 La	0 La	+.3363 L	-.2977 L	+.298 L
3	2.55	3.35	- .2225 La	- .7454 La	+.2881 L	-.3459 L	+.123 L
4	3.33	2.57	- .6125 La	-1.5741 La	+.2210 L	-.4130 L	+.200 L
5	3.89	1.62	- .8925 La	-1.4459 La	+.1393 L	-.4847 L	-.398 L
6	4.17	0.56	-1.0075 La	- .5642 La	+.0482 L	-.5858 L	-.422 L
7	4.17	-0.56	-1.0075 La	+ .5642 La	-.0482 L	-.6822 L	-.325 L
8	3.89	-1.62	- .9375 La	+1.5188 La	-.1393 L	-.7733 L	-.164 L
9	3.33	-2.57	- .7975 La	+2.0496 La	-.2210 L	-.8550 L	+.058 L
10	2.55	-3.35	- .7100 La	+2.3785 La	-.2881 L	-.9221 L	+.212 L
11	1.60	-3.91	- .7100 La	+2.7761 La	-.3363 L	-.9703 L	+.260 L
12	0.55	-4.18	- .7100 La	+2.9678 La	-.3595 L	-.9935 L	+.284 L
			-7.6075 La	+7.9254 La			

$P = -15.215\ La$ $\qquad M_y = 15.8508\ La$

$\frac{P}{A} = -.6340\ L$ $\qquad \frac{M_y}{I_y} = +0.0860\ L$

TABLE VII

4 INCH BRANCH COLUMN ANALOGY

TABULATION OF ANALYSES RESULTS

Station	Moment M							
	Analysis Number							
	5	6	7	8	9	10	11	12
1	+.199 L	+.231 L	+.278 L	+.196 L	+.236 L	+.275 L	+.180 L	+.269 L
2	+.228 L	+.255 L	+.297 L	+.229 L	+.265 L	+.298 L	+.218 L	+.294 L
3	+.067 L	+.085 L	+.113 L	+.077 L	+.102 L	+.123 L	+.072 L	+.123 L
4	-.238 L	-.233 L	-.223 L	-.215 L	-.205 L	-.200 L	-.210 L	-.195 L
5	-.354 L	-.366 L	-.377 L	-.375 L	-.382 L	-.398 L	-.359 L	-.388 L
6	-.309 L	-.338 L	-.374 L	-.357 L	-.385 L	-.422 L	-.353 L	-.431 L
7	-.186 L	-.235 L	-.296 L	-.216 L	-.265 L	-.325 L	-.219 L	-.338 L
8	-.046 L	-.067 L	-.153 L	-.057 L	-.082 L	-.164 L	-.073 L	-.170 L
9	+.058 L	+.081 L	+.053 L	+.062 L	+.080 L	+.058 L	+.058 L	+.057 L
10	+.143 L	+.153 L	+.195 L	+.160 L	+.163 L	+.212 L	+.165 L	+.217 L
11	+.204 L	+.205 L	+.234 L	+.231 L	+.223 L	+.260 L	+.243 L	+.268 L
12	+.234 L	+.230 L	+.252 L	+.265 L	+.252 L	+.284 L	+.280 L	+.293 L

FIGURE XIX

MOMENT DISTRIBUTION

Column Analogy - - 4 inch Branch

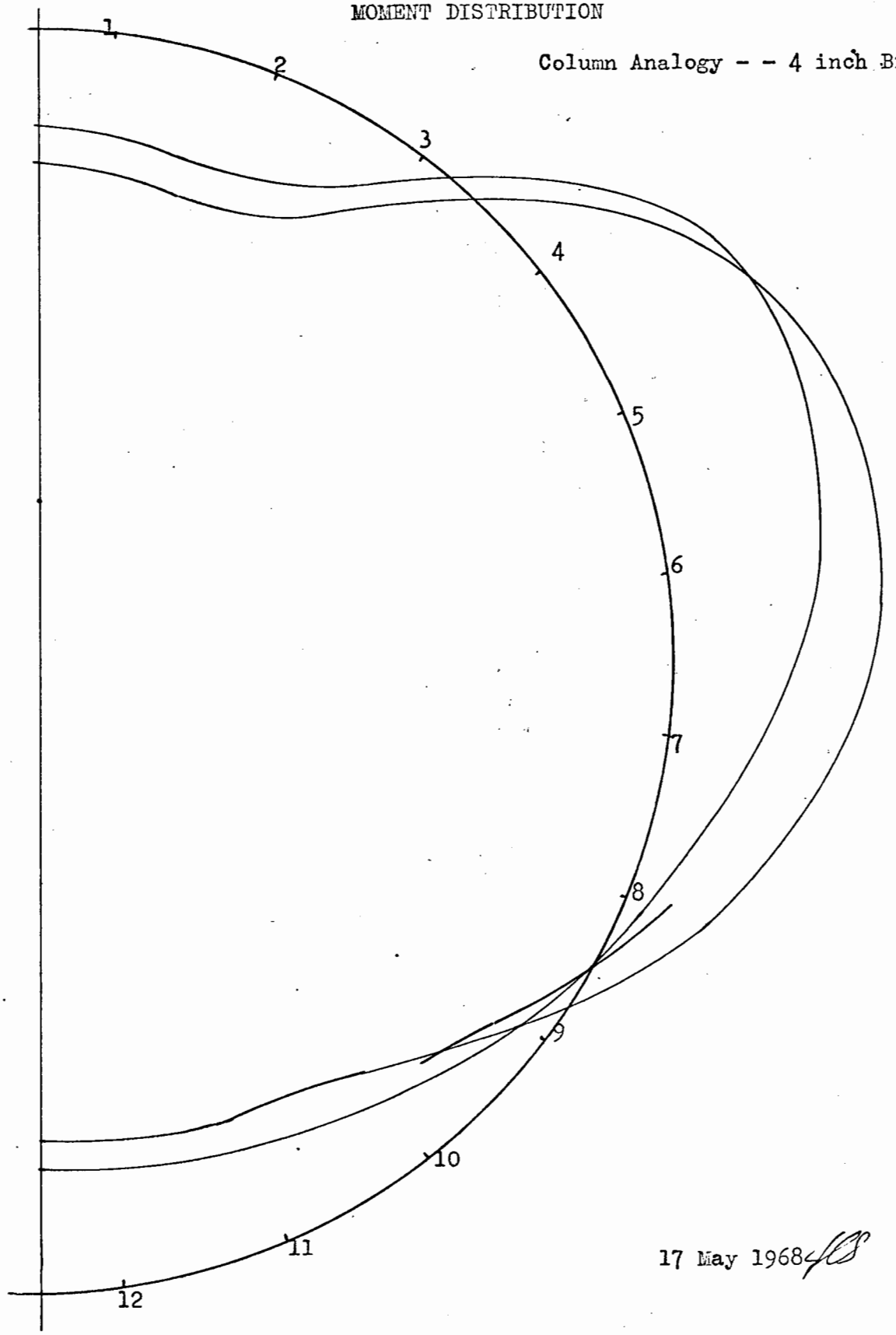

17 May 1968

where H_o and M_o are the force and moment acting on station zero with the positive directions defined as shown below in Figure XX .

Figure XX

Direction of Positive M_o H_o

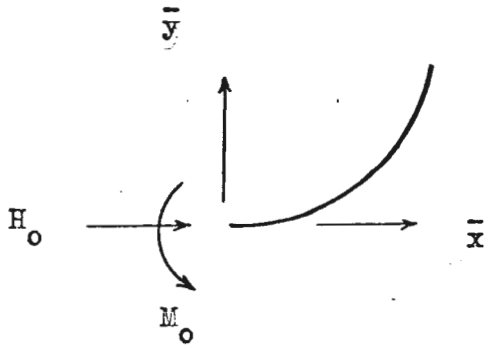

The circumferential stress at any station is given by

$$H = H_o \cos \bar{\theta} + \sum H_i : \qquad (19)$$

Tables VIII and X following show given examples of this analysis for the three and four inch branch. Tables IX and XI tabulate the results of the various analyses done with Hovgaard's and Figures XXI and XXII show the plots of these results.

STRESS PREDICTION AND COMBINATION

The stresses generated from the axial load F on the cord and thoes from the branch load L were combined in appropriate porportions to produce a difference in principal stress magitude of a given amount. This amount was obtained from preliminary tests on the photoelastic plastic as the amount of $S_1 - S_2$ which would produce the first fringe.

The stresses generated were first calculated in terms of the loads F and L. The axial load on the cord was taken as uniformly distributed

TABLE VIII

HOVGAARD'S ANALYSIS OF 3 INCH BRANCH SHOWING ANALYSIS NUMBER 1

Stat	SM	$\bar{x}$	$\bar{y}$	$\bar{y}^2$	$\bar{y}$(SM)	$\bar{y}^2$(SM)	(SM)M_B	$\bar{y}$(SM)M_B	M_B	$H_o\bar{y}$	M
0	1	0	0	0	0	0	0 L	0 L	0 L	0 L	+.206 L
1	4	1.10	0.14	0.02	0.56	0.08	0 L	0 L	0 L	-.010 L	+.196 L
2	2	2.10	0.56	0.31	1.12	0.63	0 L	0 L	0 L	-.040 L	+.163 L
3	4	2.98	1.23	1.51	4.92	6.05	0 L	0 L	0 L	-.088 L	+.117 L
4	2	3.65	2.11	4.45	4.22	8.90	-0.19 L	- .390 L	-.093 L	-.151 L	-.038 L
5	4	4.07	3.13	9.80	12.52	39.19	-0.79 L	- 2.423 L	-.198 L	-.224 L	-.021 L
6	2	4.21	4.21	17.72	8.42	35.45	-0.47 L	- 1.978 L	-.234 L	-.302 L	-.329 L
7	4	4.07	5.29	27.98	21.16	111.94	-0.79 L	- 4.179 L	-.198 L	-.379 L	-.371 L
8	2	3.65	6.31	39.82	12.62	79.63	-0.19 L	- 1.167 L	-.093 L	-.452 L	-.339 L
9	4	2.98	7.19	51.62	28.76	206.78	+0.60 L	+ 4.134 L	+.150 L	-.516 L	-.295 L
10	2	2.10	7.86	61.78	15.72	123.56	+1.18 L	+ 9.278 L	+.590 L	-.564 L	+.232 L
11	4	1.10	8.28	68.56	33.12	274.23	+3.20 L	+27.158 L	+.820 L	-.594 L	+.432 L
12	1	0	8.42	70.90	8.42	70.90	+0.82 L	+ 6.904 L	+.820 L	-.604 L	+.422 L
	Σ=36				Σ=151.56	Σ=957.38	Σ=+3.47 L	Σ=+37.484 L			

$36\ M_o + 151.56\ H_o + 3.465\ L = 0$

$151.56\ M_o + 957.3794\ H_o + 37.489\ L = 0$

$H_o = -0.0717\ L$

$M_o = +\ 0.2056\ L$

TABLE IX

3 INCH BRANCH HOVGAARD'S ANALYSIS

TABULATION OF ANALYSES RESULTS

Station	Moment M					
	Analysis Number 1	2	3	5	6	10
0	+.206 L	+.173 L	+.205 L	+.204 L	+.210 L	+.261 L
1	+.196 L	+.163 L	+.191 L	+.189 L	+.197 L	+.249 L
2	+.165 L	+.132 L	+.150 L	+.143 L	+.157 L	+.212 L
3	+.117 L	+.082 L	+.085 L	+.070 L	+.093 L	+.153 L
4	-.038 L	+.017 L	-.001 L	-.027 L	-.010 L	-.017 L
5	-.216 L	-.163 L	-.100 L	-.138 L	-.192 L	-.288 L
6	-.329 L	-.278 L	-.240 L	-.291 L	-.329 L	-.418 L
7	-.371 L	-.322 L	-.310 L	-.374 L	-.396 L	-.478 L
8	-.339 L	-.293 L	-.304 L	-.380 L	-.388 L	-.358 L
9	-.295 L	-.190 L	-.222 L	-.141 L	-.136 L	-.101 L
10	+.232 L	+.201 L	+.153 L	+.226 L	+.241 L	+.280 L
11	+.432 L	+.400 L	+.342 L	+.410 L	+.431 L	+.473 L
12	+.422 L	+.389 L	+.329 L	+.394 L	+.418 L	+.460 L

FIGURE XXI

MOMENT DISTRIBUTION

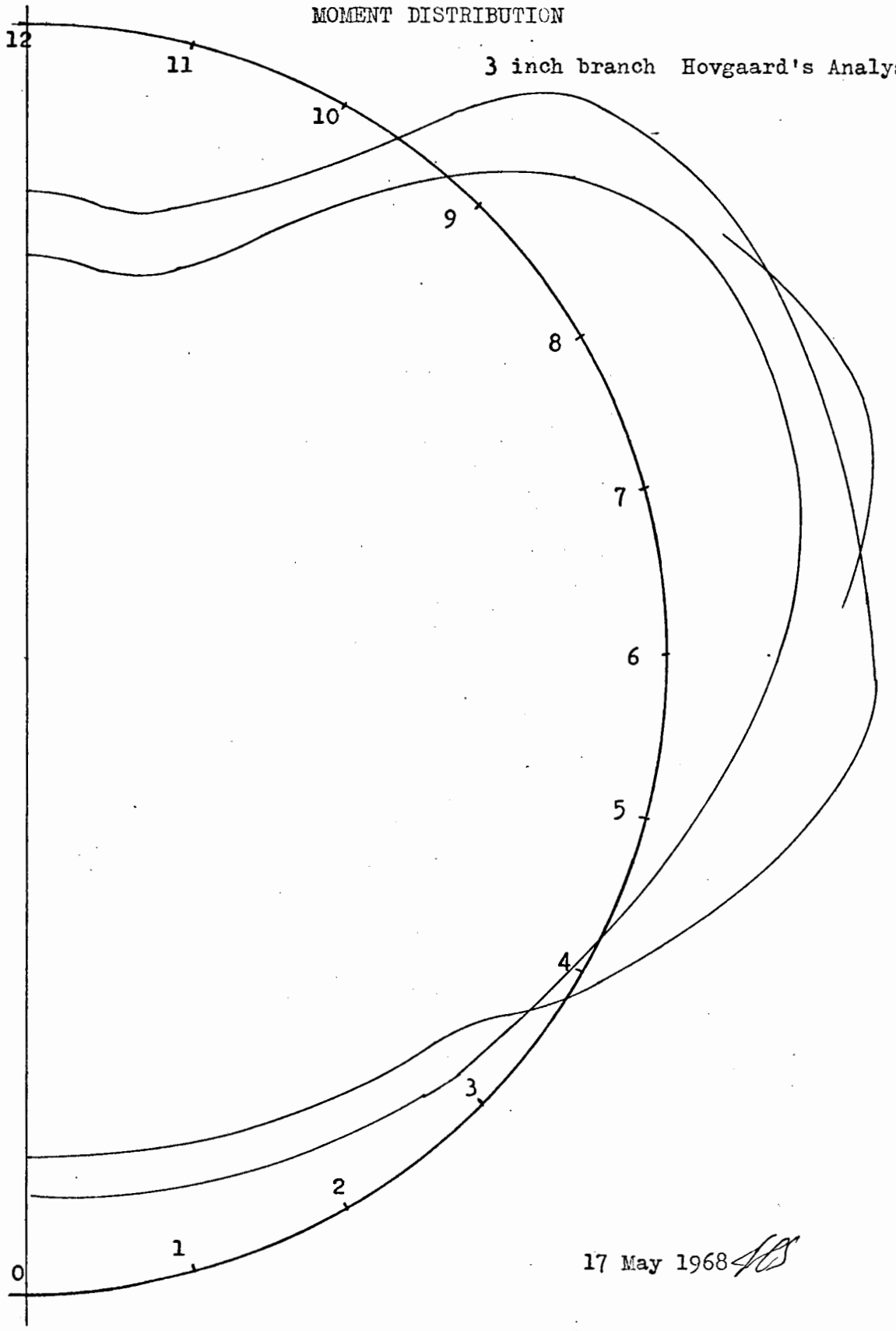

TABLE X

HOVGAARD'S ANALYSIS OF 4 INCH BRANCH SHOWING ANALYSIS NUMBER 10

Stat	SM	$\bar{x}$	$\bar{y}$	$\bar{y}^2$	$\bar{y}(SM)$	$\bar{y}^2(SM)$	$(SM)M_B$	$\bar{y}(SM)M_B$	M_B	$H_o\bar{y}$	M
0	1	0	0	0	0	0	0 L	0 L	0 L	0 L	+.231 L
1	4	1.10	0.14	0.02	0.56	0.08	0 L	0 L	0 L	-.010 L	+.220 L
2	2	2.10	0.56	0.31	1.12	0.63	0 L	0 L	0 L	-.041 L	+.190 L
3	4	2.98	1.23	1.51	4.92	6.50	0 L	0 L	0 L	-.090 L	+.141 L
4	2	3.65	2.11	4.45	4.22	8.90	-0.34 L	- .707 L	-.168 L	-.155 L	-.092 L
5	4	4.07	3.13	9.80	12.52	39.19	-1.09 L	- 3.411 L	-.273 L	-.299 L	-.271 L
6	2	4.21	4.21	17.72	8.42	35.45	-0.06 L	- 2.589 L	-.308 L	-.309 L	-.385 L
7	4	4.07	5.29	27.98	21.16	111.94	-1.09 L	- 5.766 L	-.273 L	-.388 L	-.430 L
8	2	3.65	6.31	39.82	12.62	79.63	-0.13 L	- 0.789 L	-.063 L	-.463 L	-.294 L
9	4	2.98	7.19	51.62	28.76	206.78	+1.09 L	+ 7.837 L	+.273 L	-.527 L	-.024 L
10	2	2.10	7.86	61.78	15.72	123.56	+1.42 L	+11.161 L	+.710 L	-.576 L	+.365 L
11	4	1.10	8.28	68.56	33.12	274.23	+2.84 L	+23.515 L	+.710 L	-.607 L	+.334 L
12	1	0	8.42	70.90	8.42	70.90	+0.71 L	+ 5.978 L	+.710 L	-.617 L	+.324 L
	Σ =36				Σ =151.56	Σ =957.38	Σ =+2.81 L	Σ =+35.299 L			

$36\ M_o + 151.56\ H_o + 2.805\ L = 0$

$151.56\ M_o + 957.3794\ H_o + 35.229\ L = 0$

$H_o = - 0.0733\ L$

$M_o = + 0.2307\ L$

TABLE XI

4 INCH BRANCH HOVGAARD'S ANALYSIS

TABULATION OF ANALYSES RESULTS

Station	Moment M							
	Analysis Number 5	6	7	8	9	10	11	12
0	+.173 L	+.179 L	+.208 L	+.196 L	+.202 L	+.231 L	+.206 L	+.237 L
1	+.160 L	+.168 L	+.200 L	+.181 L	+.189 L	+.220 L	+.189 L	+.223 L
2	+.120 L	+.135 L	+.175 L	+.135 L	+.150 L	+.190 L	+.139 L	+.193 L
3	+.057 L	+.081 L	+.136 L	+.026 L	+.087 L	+.141 L	+.059 L	+.140 L
4	-.026 L	-.011 L	-.089 L	-.033 L	-.004 L	-.092 L	-.046 L	-.097 L
5	-.122 L	-.175 L	-.249 L	-.144 L	-.197 L	-.271 L	-.168 L	-.282 L
6	-.258 L	-.296 L	-.348 L	-.296 L	-.334 L	-.385 L	-.296 L	-.402 L
7	-.325 L	-.347 L	-.376 L	-.379 L	-.401 L	-.430 L	-.495 L	-.412 L
8	-.316 L	-.324 L	-.331 L	-.279 L	-.287 L	-.294 L	-.267 L	-.287 L
9	-.064 L	-.059 L	-.048 L	-.040 L	-.035 L	-.024 L	-.037 L	-.021 L
10	+.310 L	+.325 L	+.350 L	+.325 L	+.340 L	+.365 L	+.321 L	+.364 L
11	+.271 L	+.292 L	+.325 L	+.279 L	+.300 L	+.334 L	+.272 L	+.331 L
12	+.258 L	+.281 L	+.317 L	+.264 L	+.287 L	+.324 L	+.254 L	+.320 L

FIGURE XXII

MOMENT DISTRIBUTION

4 inch branch Hovgaard's Analysis

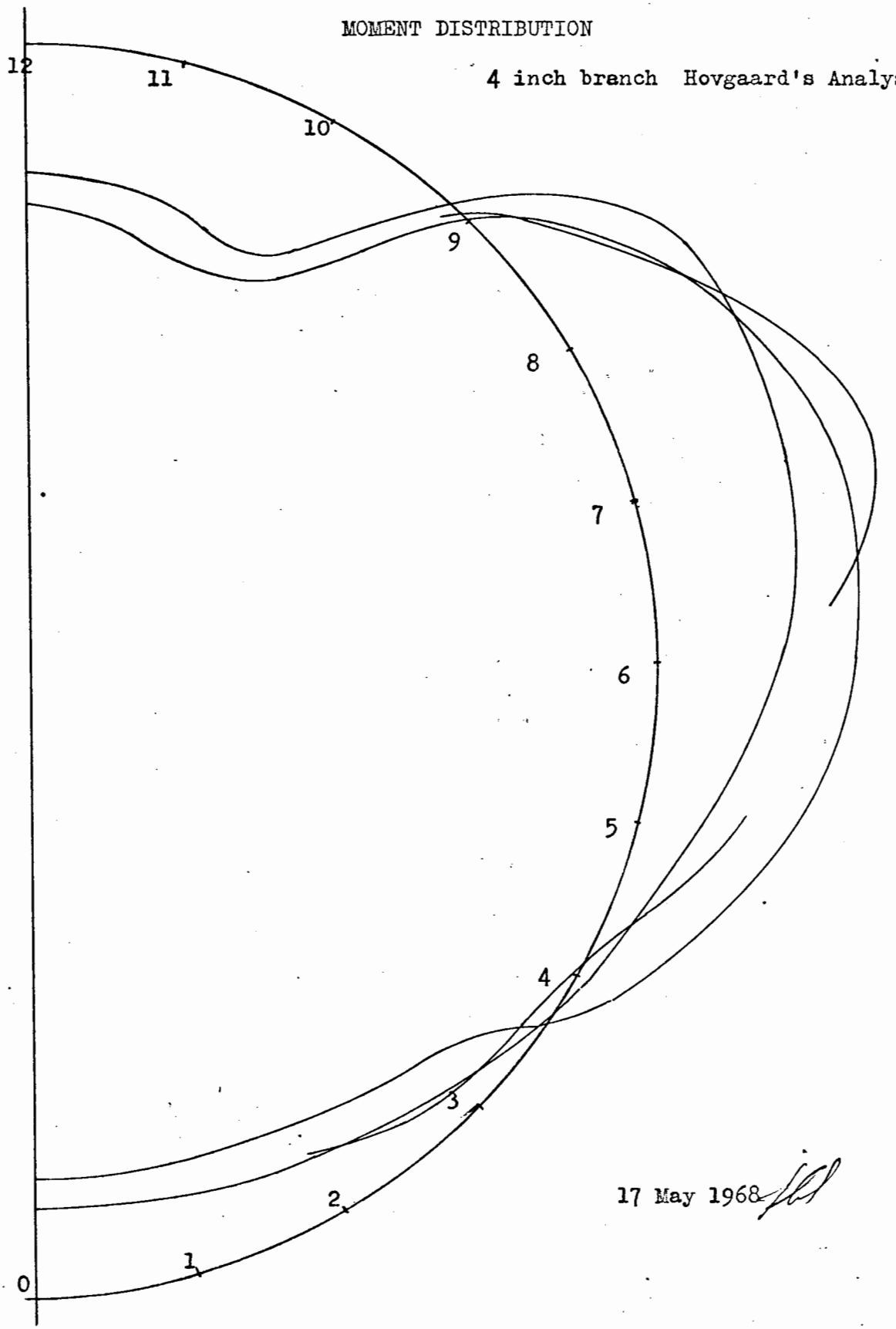

17 May 1968

around the circumference of the cord.

$$S_f = \frac{F}{A_c} \qquad (20)$$

$$= \frac{F}{19.8} = 0.0505\ F$$

The stress from the branch load L was divided into two components, that which acted perpendicular to the cord and that which acted as shear on the cord. The stress developed by the perpendicular component of the branch load was found by using the moment predicted by Hovgaard's Analysis or the Column Analogy. An average of the predicted moments was + 0.36 L for the 3 inch branch and + 0.34 L for the 4 inch branch. These analyses, as previously mentioned, used L/2 as point loads there by taking the total L load as the perpendicular component. In the 90° branch the total load did act perpendicularly to the cord but with the 45° branch only 0.707 L acted perpendicularly. Therefore in the case of the 45° branch the moments were

$$M = 0.36\ (.707\ L) = .255\ L$$

for the 3 inch branch and

$$M = .34\ (.707\ L) = .241\ L$$

for the 4 inch branch.

The stress at mid-depth of the plastic coating was calculated by

$$S_b = \frac{Mc}{I} + \frac{H}{t(1)} \qquad (21)$$

where

S_b is the stress per unit length perpendicular to the circumference

I is the moment about the neutral axis of the circumference per unit length

$$I = \frac{(1)t^3}{12}$$

t(1) is the area of the cord wall in the circumferential direction per unit length.

The H values were calculated from Hovgaard's analysis as:

$$H = H_o \text{ Cos } \bar{\theta} + \sum H_i \qquad (19)$$

and were found to be for the 3 inch branch

$$H = -.109 \text{ L Cos } 157.5^\circ + \left(\frac{L}{4} + \frac{L}{4}\right) \text{Cos } 67.5$$

$$= -.109 \text{ L } (-\text{ Sin } 67.5^\circ) + \frac{L}{2} \text{ Cos } 67.5$$

$$= .101 \text{ L} + .192 \text{ L}$$

$$= .293 \text{ L}$$

and for the 4 inch branch

$$H = -.094 \text{ L } (-\text{ Sin } 60^\circ) + \frac{L}{2} \text{ Cos } 60^\circ$$

$$= .087 \text{ L} + .25 \text{ L}$$

$$= .337 \text{ L}$$

Since each of the areas of investigation, areas (1) and (2) of Figure III, had slightly different coating thickness t_p, see Figures IX and X, it was necessary to calculate a S_b for each area and model. These S_b's are shown below in Table XII. Because of this difference in coating thickness t_p, it was also necessary to calculate the value of $S_1 - S_2$ which would produce the first fringe at each area in each model. This is also shown in Table XII.

As in the case of M being different for the 45° branch so did H exhibit the same reduction of L by .707 of its total value, so for the

3 inch branch

$$H = .293\ (.707L) = .207\ L$$

and for the 4 inch branch

$$H = .337\ (.707\ L) = .238\ L$$

TABLE XII

VALUES OF t_p, $S_1 - S_2$ FOR FIRST FRINGE APPEARENCE, S_b AND T_v

Values	Investigation Area (1) Model				Investigation Area (2)			
	3"-45°	4"-45°	3"-90°	4"-90°	3"-45°	4"-45°	3"-90°	4"-90°
t_p (inches)	.117	.114	.113	.112	.119	.119	.107	.105
S_1-S_2 (psi)	341	349	352	355	334	334	372	379
S_b (psi)	2.31L	2.20L	3.28L	3.11L	2.03L	2.18L	3.31L	3.15L
T_v (psi)	.092L	.071L	-	-	.092L	.071L	-	-

The shear load V was that component of the branch load which acted parallel to the cord centerline and was given by

$$V = L \cos \phi \qquad (22)$$

Since only two angles of ϕ were used, 45° and 90° V=0 in the case of the and V=.707 L for the 45° branch. This load was taken as exerting a pure shear to the face of the column being equal to

$$T_v = \frac{V}{C_b t} \text{ p.s.i. / inch circumference} \qquad (23)$$

$$= 0.0918 \text{ p.s.i. / inch for the 3 inch branch}$$

$$= 0.0712 \text{ p.s.i. / inch for the 4 inch branch}$$

The areas of investigation within the cord recieved this load as pure shear stress in areas (1) and (2), pure tension in (3), pure compression in (4), and areas between experiencing a combination of both shear and tension or compression.

The combination of the stresses in the 90° branch were reletively easy for

$$S_f - S_b = S_1 - S_2 \ *$$

in areas (1) and (2) and

$$S_f = (S_1 - S_2) + S_b \qquad (24)$$

For a given magitude of $S_1 - S_2$ and a given branch load. This equation (24) in terms of F and L was plotted to produce a line showing the appearence of the first fringe on a F vs L plot.

In the case of the 45° branch the combination was slightly more complex due to the added shear stress. Mohr's circle produced to formula

$$S_1 - S_2 = (4 T_v^3 + (S_f - S_b)^2)^{\frac{1}{2}} \qquad (25)$$

which is also the formula for maxim shear stress. This reduced to

$$S_f = S_b + ((S_1 - S_2)^2 - 4 T_v^2)^{\frac{1}{2}} \qquad (26)$$

---

* Normal convension defines tension as positive but this thesis the opposite was used. This was due to the defination of H_o Hovgaards Analysis as being positive when producing compression and a positive sign was carried throughout the paper for compression.

Since again a line was wanted showing the appearence of the first fringe on a plot of F vs L formula (26) was used, and also produced a straight line.

BIBLIOGRAPHY

1. Popov, E. P. ; Mechanics of Materials;p.p. 191 - 205
2. Arnott, David; Strength of Ships;Chapter VI, Principles of Naval Architecture.
3. Hovgaard, William; Structural Design of Warships; sections 14,15 and 16
4. Handbook of Experimental Stress Analysis: Hetenyi, M. (editor);
5. Filon, L. N. G.; A Manual of Photoelasticity;
6. Hendry, A. W.; An Introduction to Photoelastic Analysis
7. Redher, S.; New Methods of Photoelastic Model Investigation of Wye Manifold Branches; ASCE National Meeting on Water Resources Engineering, New York, New York, October 16 - 20; Conference Reprint 575.
8. Bouwkamp, Jack G.; Concept of Tubular Joint Design; ASCE Journal of the structural division, Volume 90 number ST2, April 1964, p.77
9. Scholl, Stanley E.; Godfrey, G. B.; Discussions of (8) above; Journal of the Structural Division, ASC, December 1964.
10. Cooper, G. W.; Hurricane Damage to Structures in the Gulf of Mexico; Ocean Industry, Oct. 1967.
11. Cross, Hardy and Mergon, N. D. ; Continuous Frames of Reinforced Concrete;
12. Johnson, L.P.; The Welded Tubular Joint Problem in Offshore Structures; SPE 484.
13. Specification for the Design, Fabrication and erection of Structural Steel for Buildings; AISC, New York, New York; April 17, 1963.
14. Godfrey, G. B.; The Allowable Stress in Axially Loaded Steel Struts; The Structural Engineer, London, England; March 1962

15. Godfrey, G. B.; Joints in Tubular Structures; The Structural Engineer, London, England; April 1959

16. Roark; Formula for Stress and Strain; p. 126

17. Bedford, T.; Welding Tubular Structurs; Welding Conference, Institution of Civil Engineers, 1953

18. Cross, H.; The Column Analogy; University of Illinois, Bulletin Number 215

19. Gerard, G. and Becker, H.; Handbook of Structural Stability Part III; NACA Technical Note 3783, Aug. 1957

20. Modern Instrumentation for Modern Stress Analysis Using the Photo-elastic Coation Technique; Photolastic Inc. Bulletin I-1100

21. Modern Photoelastic Stress Analysis; Photolastic Inc. Bulletin B-1200

22. Materials for Photoelastic Coatings, Photoelastic Models; Photolastic Inc. Bulletin P-1120

23. Surface Preparation Instructions for Bonding Photolastic Plastics; Photolastic Inc. Bulletin IB-P-110

24. Instructions for Molding and Contouring Photoelastic Sheets; Photo-lastic Inc. Bulletin IB-P-310

25. How to Select Photoelastic Coatings; Photolastic Inc. Bulletin TDP-1

26. Instructions for Bonding Flat and Contoured Photoelastic Sheets to Test Part Surfaces; Photolastic Inc. Bulletin IB-P-320

27. Photostress Large Field Meter Type LF/Z; The Budd Company, Catalog PS-2062

28. Photostress Sheet and Liquid Plastic Suggestions for Plastic Selections; Tatnall Measuring Systems Company, Bulletin BN-8022

29. Instructions for Applying Photostress Sheet Plastic with Type RCT Reflective Cement; The Budd Company, Bulletin IB-8004 Rev. 2

30. PVC TD-3 Pipe; Barrett Building Materials, A.I.A. File No. 29-B-8

31. Zandman, Felix; Photostress, Principles and Applications; Abstract from the Society of Non-Destructive Testing Handbook, 1959 Edition

32. Murray, William MacGregor; Seeing Stresses With Photo-Elasticity; ASM, Metal Progress.

33. Durelli, A.J. and Murray W.M.; Stress Distribution around a Circular Discontinuity In Any Two-Dimensional System of Combined Stress; Proceedings of the Fourteenth Semi-Annual Eastern Photoelasticity Conference, Yale University, December 6, 1941

34. Martin, Wayne D.; The design of Large Tubular Joints For Offshore Structures; Term Paper Submitted for Prof. J.H. Evans' Course 13.17 in Oceans Engineering Structures at M.I.T. Fall term 1967

35. Jones, Norman; On The Design of Pipe-Bends;Nuclear Engineering and Design 4, number 399-405, 1966.

36. Jones, N. and Kitching, R; An Experimental Investigation of A Right-Angled Single Unreinforced Mitred-Bend Subjected To Various Bending Moments; Journal Of Strain Analysis Vol. I No. 3, 1966

37. Class Notes; From Dr. W.M. Murray's Course 2.652 in Experimental Stress Analysis at M.I.T., Fall term 1967.